infected with HCV (Figure 1*D* and *F*). We detected viral protein (core) (Figure 1*B*) or viral RNA in cells (Figure 1*C*) and mouse blood by using RTD-PCR (Figure 1*D*). There was a significant reduction in the viral titers with 2-152a MAb treatment compared with that in normal IgG treatment (control) ($P < .005$, Figure 1*C* and *D*). No significant effects on body weight were observed by the inoculation of 2-152a MAb (Figure 1*E*). Further, no significant differences were found among the levels of human albumin in the sera of the normal IgG- and 2-152a MAb-inoculated mice (Figure 1*F*).

Expression of DHCR24 in Carcinoma Cells and on the Surface of HuH-7-Derived Cells

We observed abundant intracellular expression of DHCR24 in hepatoma cell lines in the previous study [12]; therefore, we characterized its expression on the surface of various carcinoma cell lines by flow cytometric analysis to clarify the mechanism of 2-152a MAb antiviral effects. In this analysis, DHCR24 expression was localized to the surface of the HuH-7 and HuH-7-based cell lines, HCV replicon cell lines (R6FLR-N, FLR3-1, and JFH-1), HCV persistently infected cell line (JFH/K4), and K4 cells; on the other hand, DHCR24 was not significantly expressed on the surface of the HepG2, Hep3B, RzM6-0d, RzM6-LC, WRL68, and PLC/PRF/5 cell lines (Supplementary Figure 1*C*). To confirm the expression of DHCR24 on the cell surface, we performed immunofluorescence staining (Supplementary Figure 1*D*). DHCR24 expression was detected in the HuH-7 cells without permeabilization.

Suppression of BGT-1 mRNA Expression in HCV Replicon Cell Lines After Treatment With 2-152a MAb

To determine the molecular mechanism underlying the effects of 2-152a MAb, we performed microarray analysis twice with different amounts of probes and evaluated the changes in gene expression associated with the 2-152a MAb treatment, which were specific to the HCV replicon cells rather than to the HCV-cured K4 cells. Using this methodology, we identified approximately 3–14 genes as upregulated and about 17–20 genes as downregulated following the treatment with 2-152a MAb, compared with the expressions in normal IgG-treated R6FLR-N, FLR3-1, and K4 cells (Figure 2*A*). Among these genes, the expression level of SLC6A12 (BGT-1; GenBank accession number NM_003044) showed significant downregulation in both the R6FLR-N and the FLR3-1 cell lines but not in the K4 cells (Figure 2*A*; Table 1). To validate this result, we tested BGT-1 mRNA expression in R6FLR-N cells treated with 2-152a MAb and normal IgG by using TaqMan expression assay. This assay

Table 1. Screened Genes in HCV Replicon Cell Lines After Treatment of IgG

	Gene name	R6FLR-N 24 hours	FLR3-1 24 hours	FLR3-1 72 hours	HuH-7/K4 24 hours
Screened specifically in replicon cells[a]					
1st screening	AKR1C1	0.67	0.62	0.65	NS
	BGT-1	0.53	0.63	0.53	NS
2nd screening	AKR1C1	0.74	NS	0.73	NS
(7-fold)[a]		or 0.75			
	F2RL2	0.72	0.68	0.62	NS
	BGT-1	0.58	0.58	0.61	NS
Screened in replicon and cured K4 cells[b]					
1st screening	CNN1	2.75	0.6	1.62	1.9
2nd screening	CNN1	2.63	2.18	1.39	1.88
(7-fold)[c]	TAGLN	1.63	1.52	1.47	1.44
	VNN2	0.65	0.63	0.66	0.67

Abbreviations: HCV, hepatitis C virus; IgG, immunoglobin G; NS, not screened.

[a] Screened genes were significantly changed in HCV replicon cells but not in HuH-7/K4 cells; each value indicates ratio of signal 2-152a MAb IgG/normal IgG treatment.

[b] Screened genes were significantly changed in all cell lines, including replicon cells and HuH-7/K4 cells.

[c] Comparing to 1st screening, 7-fold amount of labeled probe was used for microarray.

demonstrated that the relative expression of BGT-1 was significantly suppressed by the treatment with 2-152a MAb ($P < .001$, Figure 2*B*). Significant downregulation of BGT-1 was also observed by treatment with 2-152a MAb in HCV-JFH-1-infected cells (Figure 2*C*).

We further addressed the mechanism of action of 2-152a MAb. Treatment with 2-152a MAb did not decrease the level of cholesterol (Figure 2*D*), and silencing of DHCR24 did not influence BGT-1 significantly (Figure 2*E*).

Inhibition of HCV Replication and Infection by siRNA Directed Against BGT-1

Because BGT-1 expression was suppressed by the treatment with 2-152a MAb, which had antiviral activity, we attempted BGT-1 silencing in HCV replicon cell lines by using designed siRNAs to examine the potential role of BGT-1 in HCV replication. BGT-1 silencing was confirmed by RT-PCR (Figure 3*A*). The effect of the siRNAs on HCV replication was examined by Western blotting with anti-NS5A antibody (Figure 3*B*) and measured by the luminescence level (Figure 3*C*, left panel) and cell viability (Figure 3*C*, right panel) in FLR3-1 cells. We also examined the effect of these siRNAs in R6FLR-N and JFH-1 cells (Supplementary Figure 2*A*) and observed similar inhibitory effects as

Figure 2 continued. gene expression assay. Each value was compensated with values of glyceraldehyde 3-phosphate dehydrogenase (GAPDH) mRNA as the internal control and normal IgG. The asterisk indicates $P < .001$, and the vertical bars indicate the standard deviation. *C*, Level of BGT-1 and DHCR24 proteins detected in JFH/K4 cells after treatment with 2-152a or normal IgG (10 μg/mL). *D*, The relative cholesterol amount was measured in R6FLR-N cells treated with 2-152a or normal IgG (10 μg/mL). *E*, BGT-1 and DHCR24 proteins were detected in normal IgG- or 2-152a IgG-treated R6FLR-N cells.

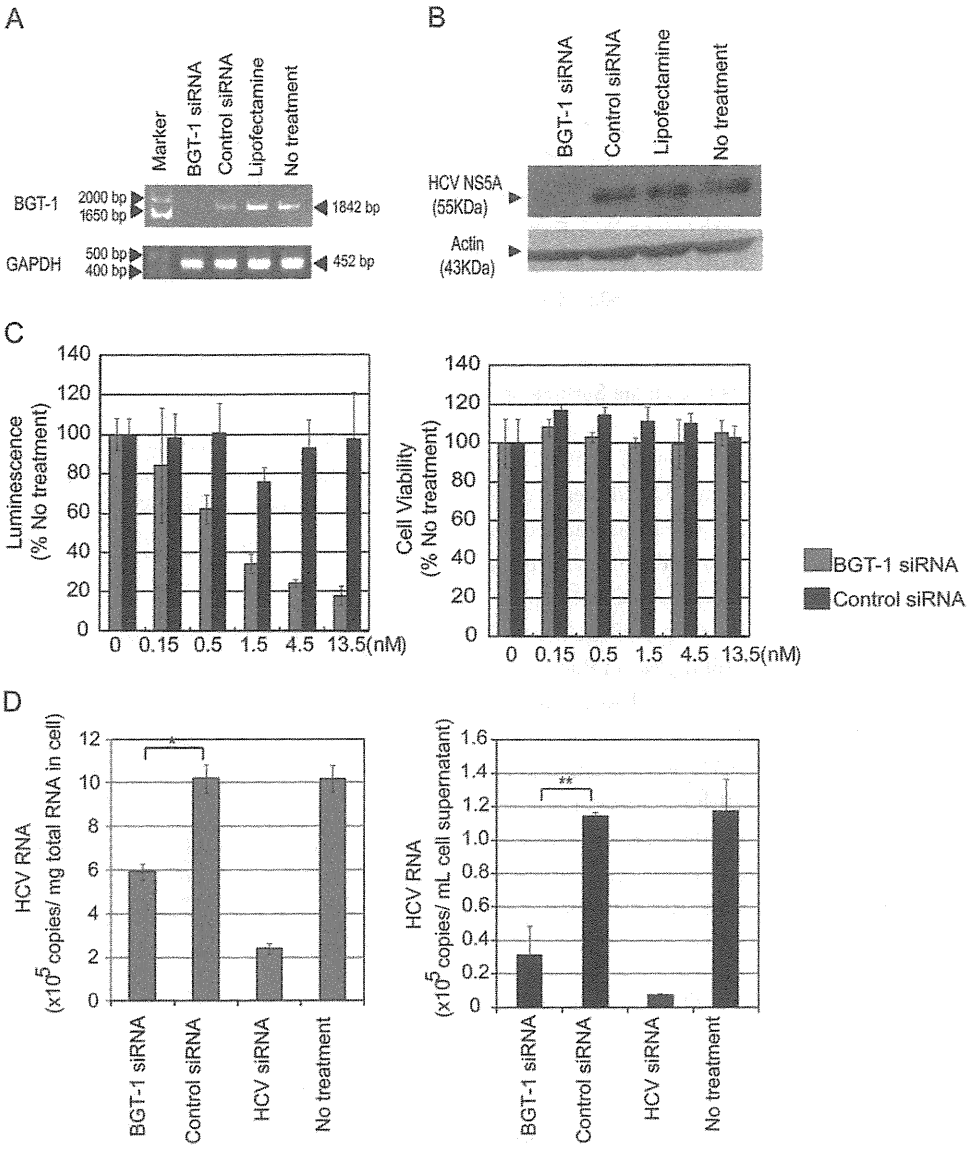

Figure 3. BGT-1 silencing by siRNA inhibits HCV replication in subgenomic HCV replicon cell lines and the persistently infected cell line. *A*, The siRNA targeting BGT-1 suppressed the expression of the corresponding mRNA. The mRNA of each sample was extracted 72 hours after siRNA (10 nM) transfection. Total RNA was transcribed and amplified by RT-PCR using primers specific to the open reading frame (ORF) of the BGT-1 (1842 bp) gene. The experiments were performed in triplicate, and the representative data are presented. *B*, The effects of BGT-1 siRNA (10 nM) on HCV were confirmed by Western blot analysis using an antibody against the HCV NS5A protein (55 kDa). The blots were striped and reprobed with an antibody directed against actin to examine protein loading in each lane. *C*, Levels of HCV replication (left panel) and cell viability (right panel) are presented according to serial concentrations of siRNA targeting BGT-1 and control siRNA in FLR3-1 cells (72 hours after transfection). The inhibition of replication or cell viability following siRNA targeting BGT-1 is defined relative to those of the cells that received no treatment (100%). The error bars represent the standard error of triplicate experiments. *D*, Quantification of HCV RNA by RTD-PCR in HCV persistently infected cells (JFH/K4) after treatment with BGT-1 siRNA. The cells were treated with siRNAs (10 nM) against BGT-1, control, and HCV (HCV R7) and harvested at 72 hours after transfection. TaqMan quantitative RT-PCR was performed for quantitation of HCV RNA in extracted RNA from cells (left panel) and their supernatants (right panel). The single asterisk (*) and double asterisk (**) indicate $P < .005$ and $P < .05$ against the control, respectively. The mean values from triplicate wells are indicated, and the vertical bars indicate the standard deviation.

those in FLR3-1 cells. The median inhibitory concentration (IC_{50}) values of BGT-1 siRNAs in various HCV replicon cell lines were as follows: FLR3-1 cells, 0.93 nM; R6FLR-N cells, 1.37 nM; JFH-1 cells, 5.95 nM. The cell viability was not significantly influenced by the siRNA treatment (Figure 3*C*, right panel; Supplementary Figure 2*A*, right panel).

Further, we monitored the levels of HCV RNA in JFH/K4 cells and their supernatants after BGT-1 silencing. Using RTD-PCR, we detected significant suppression in the HCV RNA levels by BGT-1 silencing in these cells ($P < .005$; Figure 3*D*, left panel) and their supernatants ($P < .05$; Figure 3*D*, right panel). These results were consistent with the strong inhibitory effects of

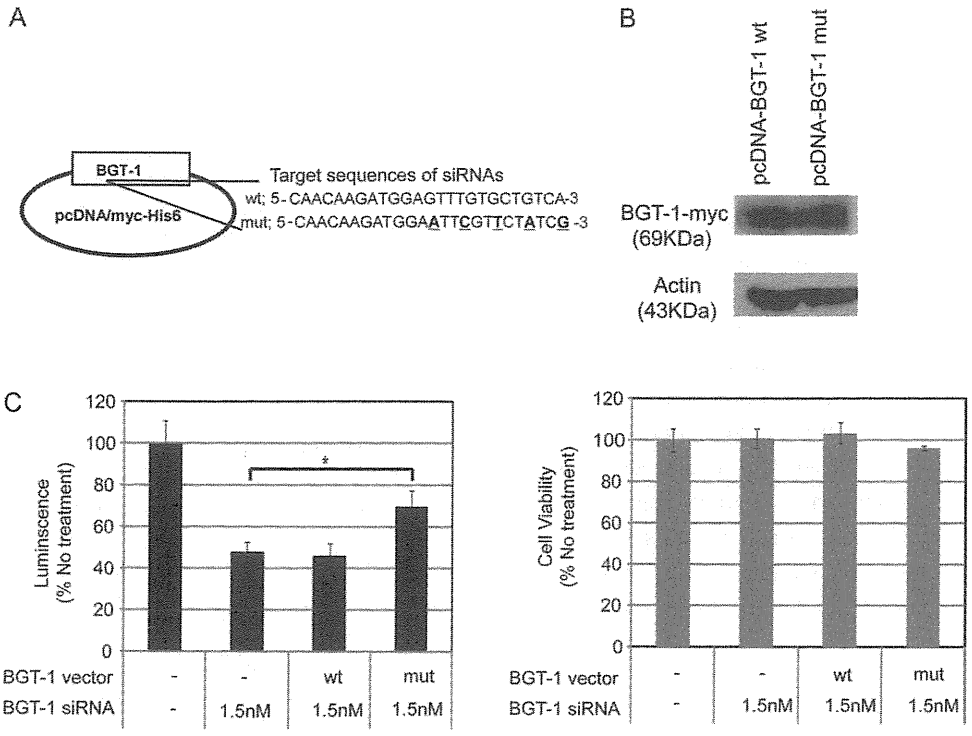

Figure 4. Validation of the inhibitory effects of BGT-1 siRNA on HCV replication in subgenomic HCV replicon cell lines. *A*, Schematic representation of the pcDNA-BGT-1 wild-type (wt) and mutant (mut) plasmids. The siRNA-targeted sites are indicated, and the underlined bold letters indicate the sequences induced by mutagenesis PCR. *B*, The wild type and mutant of the BGT-1-myc fusion protein were detected by using an anti-myc monoclonal antibody (9E10) in transfected R6FLR-N cells (upper panel). The blots were striped and reprobed with an antibody against actin to determine protein loading for each lane (lower panel). *C*, R6FLR-N cells were transfected with BGT-1 siRNA, and wild-type or mutant expression vectors were transfected after siRNA transfection. After 24 hours of vector transfection, the level of HCV replication (left panel) was measured by luminescence, and cell viability (right panel) was measured by WST-8 assay. The asterisk indicates $P < .05$ compared with transfection of siRNA alone. The mean values from triplicate wells are indicated, and the vertical bars represent the standard deviation.

BGT-1 siRNA on HCV replication, as shown in Figure 3*C*. We designed alternative siRNA targeting BGT-1 (BGT-1-siRNA-362) and observed its significant inhibitory effect on HCV replication without significant cytotoxicity (Supplementary Figure 2*B*).

Validation of the Anti-HCV Effects of siRNA Against BGT-1 by Rescue With Expression Vectors

To assess the specificity of BGT-1 silencing, we attempted to rescue HCV replication against the ectopic effects by this silencing. To examine the effect of the rescue, we constructed expression vectors of wild-type and mutant BGT-1 (Figure 4*A*) and confirmed the expression of each BGT-1-myc-fused protein (Figure 4*B*). The mutant BGT-1 vector contained 5 base mismatches within the site targeted by the BGT-1 siRNA without a change in the amino acid sequence of the protein (underlined in Figure 4*A*). We also transfected the pcDNA-BGT-1 plasmid after the siRNA treatment and observed significant recovery of HCV replication with mutant pcDNA-BGT-1 ($P < .05$; Figure 4*C*, left panel) without significant cytotoxicity (Figure 4*C*, right panel). BGT-1 expression was increased significantly in K4 cells in the presence of HCV ($P < .05$, Supplementary Figure 2*C*) at 72 hours after infection compared with the absence of HCV, and in RzM6-LC cells, which persistently express HCV [8], compared with RzM6-0d cells, which lack HCV expression ($P < .05$, Supplementary Figure 2*D*).

DISCUSSION

In this study, we determined that 2-152a MAb, which binds to but does not affect the activity of DHCR24, suppresses HCV replication and that BGT-1 is highly downregulated in HCV replicon cell lines treated with this antibody. Further, the efficient rescue of viral replication with a mutant expression vector indicates the specific inhibitory effect of BGT-1 silencing on HCV replication. Therefore, we hypothesize that BGT-1 plays an important role in HCV replication through a pathway that is likely independent of DHCR24, which in its own right can regulate the HCV life cycle [13].

BGT-1 is involved in sodium- and chloride-coupled betaine uptake, which helps in maintaining normal cellular conditions. Previous reports have described that the transcription of BGT-1 mRNA is regulated by a tonicity sensitive element (TonE) in response to hypertonic stress, a result that was first identified in the Madin-Darby canine kidney (MDCK) cell line [24]. BGT-1

is also thought to be responsible for the hyperosmotic stress response and in maintaining cell hydration. Denkert et al [25] reported that BGT-1 gene expression is induced by hyperosmolarity and inhibited by p38 mitogen-activated protein kinase ($p38^{MAPK}$) inhibitor SB20358. Further, several reports have evidenced that cell hydration affects viral replication and that viral replication increases during cell shrinkage due to hyperosmolarity, a result that was accompanied by increased BGT-1 mRNA expression [26]. Considering the reduction in HCV replication by the BGT-1 siRNA treatment, this treatment may prevent HCV replication by affecting hypoosmotic conditions in HCV-infected cells. Further studies are required to examine in detail the function of BGT-1 in HCV replication.

In summary, we demonstrated that the 2-152a monoclonal antibody inhibits HCV replication in HCV replicon cells and HCV infection in human hepatocytes transplanted into chimeric mice. The inhibitory effect of the monoclonal antibody on viral replication may be mediated by the suppression of BGT-1 expression. We propose BGT-1 as a key target for anti-HCV therapies.

Supplementary Data

Supplementary materials are available at *The Journal of Infectious Diseases* online (Supplementary Data).

Supplementary materials consist of data provided by the author that are published to benefit the reader. The posted materials are not copyedited. The contents of all supplementary data are the sole responsibility of the authors. Questions or messages regarding errors should be addressed to the author.

Notes

Acknowledgments. The authors thank I. Maruyama, K. Tanaka, T. Seki, and R. Takehara for their excellent technical support, and Y. Tokunaga for the insightful comments and helpful discussion.

Financial Support. This work was supported by grants from the Ministry of Health and Welfare of Japan; Ministry of Education, Culture, Sports, Science and Technology of Japan; Program for Promotion of Fundamental Studies in Health Sciences of the National Institute of Biomedical Innovation; and Cooperative Research Project on Clinical and Epidemiological Studies of Emerging and Reemerging Infectious Diseases.

Potential conflicts of interest. All authors: No reported conflicts.

All authors have submitted the ICMJE Form for Disclosure of Potential Conflicts of Interest. Conflicts that the editors consider relevant to the content of the manuscript have been disclosed.

References

1. Di Bisceglie AM, Carithers RL Jr, Gores GJ. Hepatocellular carcinoma. Hepatology **1998**; 28:1161–5.
2. Hayashi J, Aoki H, Arakawa Y, Hino O. Hepatitis C virus and hepatocarcinogenesis. Intervirology **1999**; 42:205–10.
3. Michielsen PP, Francque SM, van Dongen JL. Viral hepatitis and hepatocellular carcinoma. World J Surg Oncol **2005**; 3:27.
4. Mazzella G, Accogli E, Sottili S, et al. Alpha interferon treatment may prevent hepatocellular carcinoma in HCV-related liver cirrhosis. J Hepatol **1996**; 24:141–7.
5. Bruchfeld A, Stahle L, Andersson J, Schvarcz R. Ribavirin treatment in dialysis patients with chronic hepatitis C virus infection—a pilot study. J Viral Hepat **2001**; 8:287–92.
6. Kohara M, Tanaka T, Tsukiyama-Kohara K, et al. Hepatitis C virus genotypes 1 and 2 respond to interferon-alpha with different virologic kinetics. J Infect Dis **1995**; 172:934–8.
7. Nakamura H, Ogawa H, Kuroda T, et al. Interferon treatment for patients with chronic hepatitis C infected with high viral load of genotype 2 virus. Hepatogastroenterology **2002**; 49:1373–6.
8. Tsukiyama-Kohara K, Toné S, Maruyama I, et al. Activation of the CKI-CDK-Rb-E2F pathway in full genome hepatitis C virus-expressing cells. J Biol Chem **2004**; 279:14531–41.
9. Crameri A, Biondi E, Kuehnle K, et al. The role of seladin-1/DHCR24 in cholesterol biosynthesis, APP processing and Aβ generation in vivo. EMBO J **2006**; 25:432–43.
10. Waterham HR, Koster J, Romeijn GJ, et al. Mutations in the 3β-hydroxysterol Δ^{24}-reductase gene cause desmosterolosis, an autosomal recessive disorder of cholesterol biosynthesis. Am J Hum Genet **2001**; 69:685–94.
11. Lu X, Kambe F, Cao X, et al. 3β-Hydroxysteroid-Δ24 reductase is a hydrogen peroxide scavenger, protecting cells from oxidative stress-induced apoptosis. Endocrinology **2008**; 149:3267–73.
12. Nishimura T, Kohara M, Izumi K, et al. Hepatitis C virus impairs p53 via persistent overexpression of 3β-hydroxysterol Δ24-reductase. J Biol Chem **2009**; 284:36442–52.
13. Takano T, Tsukiyama-Kohara K, Hayashi M, et al. Augmentation of DHCR24 expression by hepatitis C virus infection facilitates viral replication in hepatocytes. J Hepatol **2011**; 55:512–21.
14. Lohmann V, Körner F, Koch J, Herian U, Theilmann L, Bartenschlager R. Replication of subgenomic hepatitis C virus RNAs in a hepatoma cell line. Science **1999**; 285:110–3.
15. Watanabe T, Sudoh M, Miyagishi M, et al. Intracellular-diced dsRNA has enhanced efficacy for silencing HCV RNA and overcomes variation in the viral genotype. Gene Ther **2006**; 13:883–92.
16. Sakamoto H, Okamoto K, Aoki M, et al. Host sphingolipid biosynthesis as a target for hepatitis C virus therapy. Nat Chem Biol **2005**; 1:333–7.
17. Kato T, Date T, Miyamoto M, et al. Efficient replication of the genotype 2a hepatitis C virus subgenomic replicon. Gastroenterology **2003**; 125: 1808–17.
18. Blight KJ, McKeating JA, Rice CM. Highly permissive cell lines for subgenomic and genomic hepatitis C virus RNA replication. J Virol **2002**; 76:13001–14.
19. Wakita T, Pietschmann T, Kato T, et al. Production of infectious hepatitis C virus in tissue culture from a cloned viral genome. Nat Med **2005**; 11:791–6.
20. Mercer DF, Schiller DE, Elliott JF, et al. Hepatitis C virus replication in mice with chimeric human livers. Nat Med **2001**; 7:927–33.
21. Inoue K, Umehara T, Ruegg UT, et al. Evaluation of a cyclophilin inhibitor in hepatitis C virus-infected chimeric mice in vivo. Hepatology **2007**; 45:921–8.
22. Takeuchi T, Katsume A, Tanaka T, et al. Real-time detection system for quantification of hepatitis C virus genome. Gastroenterology **1999**; 116:636–42.
23. Sarkar D, Imai T, Kambe F, et al. The human homolog of Diminuto/Dwarf1 gene (hDiminuto): a novel ACTH-responsive gene overexpressed in benign cortisol-producing adrenocortical adenomas. J Clin Endocrinol Metab **2001**; 86:5130–7.
24. Takenaka M, Preston AS, Kwon HM, Handler JS. The tonicity-sensitive element that mediates increased transcription of the betaine transporter gene in response to hypertonic stress. J Biol Chem **1994**; 269: 29379–81.
25. Denkert C, Warskulat U, Hensel F, Häussinger D. Osmolyte strategy in human monocytes and macrophages: involvement of p38MAPK in hyperosmotic induction of betaine and myoinositol transporters. Arch Biochem Biophys **1998**; 354:172–80.
26. Häussinger D. The role of cellular hydration in the regulation of cell function. Biochem J **1996**; 313:697–710.

Research Article

EASL EUROPEAN ASSOCIATION FOR THE STUDY OF THE LIVER | JOURNAL OF HEPATOLOGY

Augmentation of DHCR24 expression by hepatitis C virus infection facilitates viral replication in hepatocytes

Takashi Takano[1,†], Kyoko Tsukiyama-Kohara[2,*], Masahiro Hayashi[1], Yuichi Hirata[1], Masaaki Satoh[2], Yuko Tokunaga[1], Chise Tateno[3], Yukiko Hayashi[4], Tsunekazu Hishima[4], Nobuaki Funata[4], Masayuki Sudoh[5], Michinori Kohara[1]

[1]*Department of Microbiology and Cell Biology, Tokyo Metropolitan Institute of Medical Science, 2-1-6 Kamikitazawa, Setagaya-ku, Tokyo 156-8506, Japan;* [2]*Department of Experimental Phylaxiology, Faculty of Medical and Pharmaceutical Sciences, Kumamoto University, 1-1-1 Honjo, Kumamoto, Kumamoto 860-8556, Japan;* [3]*Phoenix Bio Co., Ltd., Study Service Department, 3-4-1 Kagamiyama, Higashi-Hiroshima 739-0046, Japan;* [4]*Department of Pathology, Tokyo Metropolitan Komagome Hospital, 3-18-22 Honkomagome, Bunkyo-ku, Tokyo 113-8677, Japan;* [5]*Kamakura Research Laboratories, Chugai Pharmaceutical Co., Ltd., Kajiwara 200, Kamakura-City, Kanagawa 247-8530, Japan*

Background & Aims: We characterized the role of 24-dehydrocholesterol reductase (DHCR24) in hepatitis C virus infection (HCV). DHCR24 is a cholesterol biosynthetic enzyme and cholesterol is a major component of lipid rafts, which is reported to play an important role in HCV replication. Therefore, we examined the potential of DHCR24 as a target for novel HCV therapeutic agents.

Methods: We examined DHCR24 expression in human hepatocytes in both the livers of HCV-infected patients and those of chimeric mice with human hepatocytes. We targeted *DHCR24* with siRNA and U18666A which is an inhibitor of both DHCR24 and cholesterol synthesis. We measured the level of HCV replication in these HCV replicon cell lines and HCV infected cells. U18666A was administrated into chimeric mice with humanized liver, and anti-viral effects were assessed.

Results: Expression of DHCR24 was induced by HCV infection in human hepatocytes *in vitro*, and in human hepatocytes of chimeric mouse liver. Silencing of *DHCR24* by siRNA decreased HCV replication in replicon cell lines and HCV JFH-1 strain-infected cells. Treatment with U18666A suppressed HCV replication in the replicon cell lines. Moreover, to evaluate the anti-viral effect of U18666A *in vivo*, we administrated U18666A with or without pegylated interferon to chimeric mice and observed an inhibitory effect of U18666A on HCV infection and a synergistic effect with interferon.

Conclusions: DHCR24 is an essential host factor which augmented its expression by HCV infection, and plays a significant role in HCV replication. DHCR24 may serve as a novel anti-HCV drug target.

Introduction

Extensive epidemiological studies have identified multiple risk factors for hepatocellular carcinoma (HCC), including chronic infection with hepatitis C virus (HCV), and hepatitis B virus (HBV), and cirrhosis due to non-viral etiologies, such as alcohol abuse and aflatoxin B1 exposure [1,2]. Of these factors, HCV appears to be the dominant causative factor for HCC in many developed countries. The World Health Organization estimates that 170 million people worldwide are infected with HCV and are, therefore, at risk of developing liver cirrhosis and HCC [3]. The combination of pegylated interferon-α (PEG-IFN-α) and ribavirin is currently the standard treatment regimen for patients with chronic HCV infection. However, viral clearance is achieved in only 40% to 60% of patients and depends on the HCV genotype with which the patient is infected [4].

We previously established the RzM6 cell line, a HepG2 cell line in which the full-length HCV genome (HCR6-Rz) can be conditionally expressed under control of the Cre/*lox*P system and is precisely self-trimmed at the 5′ and 3′-termini by ribozyme sequences [5]. Anchorage-independent growth of these cells accelerates after 44 days of continuous passaging, during which the Cdk-Rb-E2F pathway is activated [5]. In a previous study, we developed monoclonal antibodies (MoAbs) against cell surface antigens on HCV-expressing cells that had been passaged for over 44 days [6]. One of the targets of these MoAbs was 24-dehydrocholesterol reductase (DHCR24 is also called 3-β-hydroxysterol-Δ-24-reductase, seladin-1, desmosterol delta-24-reductase), a molecule that is frequently overexpressed in the hepatocytes of HCV-infected patients.

Keywords: Hepatitis C virus; Replication; DHCR24; U18666A.
Received 18 April 2010; received in revised form 11 November 2010; accepted 2 December 2010; available online 22 December 2010

* Corresponding author. Address: Department of Experimental Phylaxiology, Faculty of Life Sciences, Kumamoto University, 1-1-1 Honjo, Kumamoto, Kumamoto 860-8556, Japan. Tel./fax: +81 96 373 5560.
E-mail address: kkohara@kumamoto-u.ac.jp (K. Tsukiyama-Kohara).
† Present address: Division of Veterinary Public Health, Nippon Veterinary and Life Science University, 1-7-1 Kyonan, Musashino, Tokyo 180-8602, Japan.

Abbreviations: DHCR24, 24-dehydrocholesterol reductase; HCV, hepatitis C virus; MoAb, monoclonal antibody; HCC, hepatocellular carcinoma; HBV, hepatitis B virus.

ELSEVIER

Journal of Hepatology **2011** vol. 55 | 512–521

DHCR24 confers resistance to apoptosis in neuronal cells [7]. It also regulates the cellular response to oxidative stress by binding to the amino terminus of p53, thereby displacing mouse double minute 2 homolog isoform MDM2 (*Homo sapiens*) (MDM2) from p53 and inducing the accumulation of p53 in human embryonic fibroblasts [8].

DHCR24 is a cholesterol biosynthetic enzyme that is also called desmosterol reductase [9,10]. Cholesterol is a major component of lipid rafts, which are reported to play an important role in HCV replication [11]. Therefore, we characterized the role of DHCR24 in HCV replication and evaluated its potential as a target for novel HCV therapeutic agents. We also examined the synergistic antiviral effect of U18666A which is an inhibitor of both DHCR24 [12] and cholesterol synthesis [13] with IFN-α in the treatment of HCV.

Materials and methods

Cells and plasmids

Cell culture methods of the HuH-7 [14], HepG2 [15], hybridoma and myeloma PAI cells, RzM6 cells [5], and the HCV subgenomic replicon cells lines FLR3-1 (genotype 1b, strain Con-1; [16]), R6FLR-N (genotype 1b, strain N; [17]), and Rep JFH Luc3-13) genotype 2a, strain JFH-1 [18]) were utilized to evaluate HCV replication [19] are described in Supplementary data.

The *DHCR24* cDNA was synthesized and amplified by PCR using Phusion™ DNA polymerase (Finnzymes) and cloned into the pcDNA3.1 vector (Invitrogen) or lentivirus vector, as described previously [6].

Matrix-assisted laser desorption ionization time-of-flight mass spectrometry analysis

The detailed procedures are described in Supplementary data [20].

Immunohistochemistry and Western blot analysis

The detailed procedures are described in Supplementary data.

The antibodies used in this experiment were: anti-Core, anti-NS3, anti-NS4B, anti-NS5B [5], and anti-NS5A (kindly provided by Dr. Matsuura, Osaka University), and anti-actin (Sigma).

Inhibition of DHCR24 by siRNA

We synthesized two siRNAs that were directed against human *DHCR24* mRNA: siDHCR24-417 and siDHCR24-1024. The target sequence of siDHCR24-417 was 5′-GUACAAGAAGACACACAAATT-3′, while that of siDHCR24-1024 was 5′-GAGAACUAUCUGAAGACAATT-3′. Additionally, we used siRNAs targeted against the HCV genome (siE-R7 and siE-R5) [17,21]. The siCONTROL Non-Targeting siRNA #3 (Dharmacon RNA Technologies) was used as the negative control siRNA. The chemically synthesized siRNAs were transfected into cells using Lipofectamine RNAiMAX (Invitrogen) and Opti-MEM (Invitrogen) by reverse-transfection. Cells were characterized 72 h after transfection.

Inhibition of viral replication by U18666A

U18666A (Calbiochem) was utilized to treat HCV replicon cells at a concentration of 62.5–1000 nM and chimeric mice at a concentration of 10 mg/kg (i.p.).

To determine whether cholesterol can reverse the U18666A treatment by the addition of cholesterol, we performed the experiments using HCV replicon cells (4×10^3 cells/well in a 96-well white plate, SUMILON). Culture medium was replaced after the cells had spread (at 24 h), and LDL (Calbiochem) was added to reach a final cholesterol concentration of 50 μg/ml. After a 24 h-incubation, U18666A (62.5, 125, 250, 500, and 1000 nM) was added to each well, and the cells were incubated for an additional 48 h. HCV replication activity was measured by luciferase assay, and cell viability was measured with the WST-8 cell counting kit according to the manufacturer's instructions (Dojindo Laboratories). Cholesterol measurements are described in Supplementary data.

Inhibition assay of HCV replication in replicon cells and persistent infected cells

For evaluation of the anti-HCV replication effect of the inhibitor U18666A in replicon cells and HCV persistently infected cells are described in Supplementary data.

Real-time detection (RTD)-PCR

Total RNA was purified from JFH-K4 cells that had been treated with siRNA or U18666A by the acid guanidium–phenol–chloroform method. HCV RNA was quantified by RTD-PCR as previously described [22].

HCV infection of chimeric mice with humanized liver and mRNA quantification by RTD-PCR

We used chimeric mice that were created by transplanting human primary hepatocytes into severe combined immunodeficient mice carrying a urokinase plasminogen activator transgene [23,24] that was controlled by the albumin promoter. These hepatocytes had been infected with plasma from a HCV-positive patient HCR6 (genotype 1b) [19]. The HCV 1b RNA level reached 2.9–18.0 × 10^6 copies/ml in mouse sera after 1–2 months of infection. HCV RNA in the mouse serum or total RNA from liver tissue from humanized chimeric mice with/without HCV infection was extracted using the acid guanidium–phenol–chloroform method. HCV RNA and *DHCR24* mRNA levels were quantified by RTD-PCR [22]. The primers and probes for HCV were prepared as previously described [22], and the primers and probes for *DHCR24* were prepared using TaqMan® Gene Expression assays (Applied Biosystems) according to the manufacturer's instructions. PEG-IFNα-2a (Chugai) was administered subcutaneously at a concentration of 30 μg/kg, at day 1, 4, 8, and 11 (the amount of PEG-IFN-α administered to the chimeric mice was 20-fold relative to that used in humans), and U18666A was administered intraperitoneally at a concentration of 10 mg/kg, every day for 2 weeks (Fig. 6A). The protocols for the animal experiments were approved by the local ethics committee.

Human serum albumin in the blood of humanized chimeric mice was measured using a commercially available kit, according to the manufacturer's instructions (Alb-II kit; Eiken Chemical).

Results

Identification of DHCR24

We inoculated mice (BALB/c) with RzM6 cells that expressed HCV protein and had been cultured for over 44 days (denoted as RzM6-LC cells); mice were inoculated at least seven times over a 2-week period. We then fused the splenocytes from mice that had been immunized with RzM6-LC cells to myeloma cells to establish hybridomas. Characterization of the culture supernatant from more than 1000 hybridoma cells by ELISA (data not shown) revealed that one MoAb clone (2-152a) recognized a molecule of approximately 60 kDa in various cells (Supplementary Fig. 1A and B. This molecule was more highly expressed in RzM6-LC cells (Supplementary Fig. 1A), HeLa cells, and HCC cell lines (HepG2, HuH-7, Hep3B, and PLC/PRF/5) than in HEK293 cells and several normal liver cell lines (NKNT, TTNT, and WRL68) (Supplementary Fig. 1B). To further characterize this molecule, we performed matrix-assisted laser desorption ionization time-of-flight mass spectrometry (MALDI-TOF-MS) and obtained seven peptide sequences (Supplementary Fig. 1C, underlined). These peptide sequences suggested that the molecule that was recognized by the 2-152a antibody was DHCR24. We constructed a lentivirus expression vector containing myc-tagged DHCR24 (DHCR24-myc) and transduced it into HepG2 cells. By western blot analysis with 2-152a and anti-Myc antibody, we then confirmed that DHCR24 was expressed in the transduced cells (Supplementary Fig. 1D). We found that the 2-152a antibody specifically recognized DHCR24.

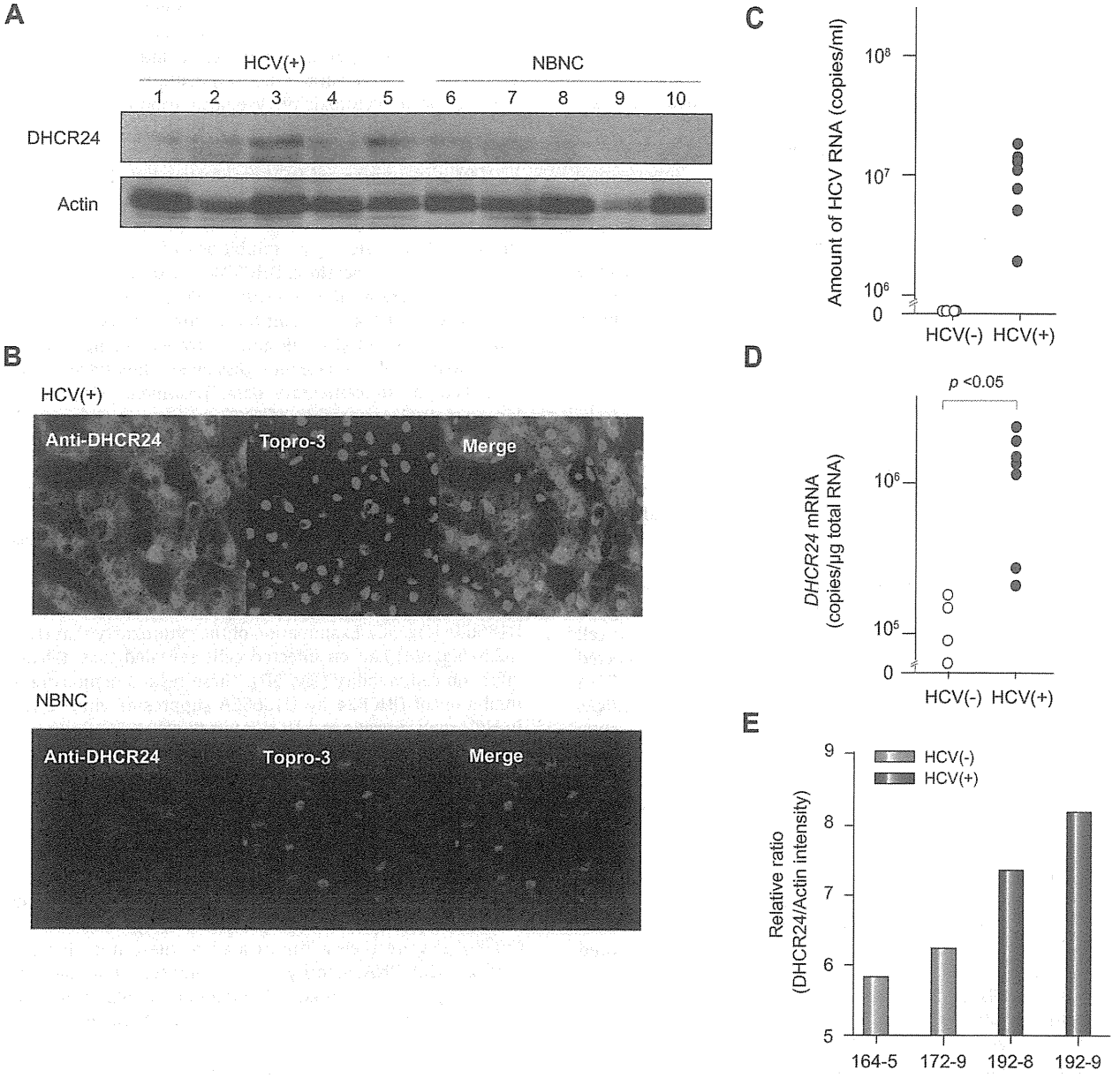

Fig. 1. HCV induces DHCR24 overexpression *in vitro* and *in vivo*. (A) Expression of DHCR24 in non-cancerous regions of livers of HCV-infected (+) and NBNC-HCC patients. Lysates (25 μg/lane) of non-cancerous liver tissues from HCC patients were analyzed by Western blot analysis using MoAb 2-152a. The patient numbers (Supplementary Table 1) are indicated at the top of the blot. (B) Immunohistochemical staining of HCV-infected non-cancerous tissues derived from an HCC patient using the monoclonal antibody 2-152a (Alexa488), anti-TO-PRO-3, or a merge (600× magnification) (upper panel). Tissues from an NBNC patient stained with the monoclonal antibody 2-152a (Alexa488) as well as TO-PRO-3 (640× magnification) (lower panel). (C) The amount of HCV RNA that was present in the HCV-R6 (genotype 1b)-infected chimeric mice with the humanized liver was quantified using RTD-PCR. The results of HCV uninfected ($n = 4$) and infected ($n = 7$) is indicated. (D) The amount of *DHCR24* mRNA present in total RNA isolates of HCV-R6 (genotype 1b)-infected chimeric mice with the humanized liver was quantified using RTD-PCR. $^*p < 0.05$ (Mann–Whitney test). The results of HCV uninfected ($n = 4$) and infected ($n = 7$) are indicated. (E) DHCR24 protein was detected by Western blot analysis using MoAb 2-152a as a probe, and quantitated by LAS3000. Protein levels are normalized to actin and ratio is indicated.

HCV infection in vivo induces persistent overexpression of DHCR24

We next examined whether HCV infection could induce DHCR24 expression in human hepatocytes. DHCR24 was overexpressed more frequently in liver tissues from HCV-positive patients than in tissues from HBV- and HCV-negative (NBNC) patients (Fig. 1A and Supplementary Table 1). The liver tissue from HCV-positive patients stained more strongly for DHCR24 expression than the liver tissue from NBNC patients (Fig. 1B). We inoculated chimeric mice [19,23,25] with HCV ($10^{6.2}$ copies/ml) that had been isolated from the plasma of HCV-infected patients (patient R6, HCV genotype 1b). The serum concentration of human albumin (Supplementary Fig. 2A) in the chimeric mice after transplantation of hepatocytes indicated that human hepatocytes had engrafted in the mouse livers. Thirty days after transplantation, mice were infected with HCV, and HCV and RNA titers were analyzed both

before and after inoculation (Supplementary Fig. 2B). The average amount of HCV RNA that was present in the serum of the infected chimeric mice at 28 days post-infection was 1.1×10^7 copies/ml (Fig. 1C and Supplementary Fig. 2B). The *DHCR24* mRNA levels in the livers of the chimeric mice were also quantified at 28 days post-infection by real-time detection (RTD)-PCR [22]. The results revealed that there was a significant increase in *DHCR24* expression as measured by mRNA levels in HCV infected chimeric mice (Fig. 1D). Next, we examined the extent to which translation of DHCR24 occurred in the chimeric mice (Fig. 1E), higher DHCR24 protein levels were present in hepatocytes from HCV-infected mice (Nos. 192-8 and 192-9) than in those of uninfected mice (Nos. 164-5 and 172-9). These findings indicate that expression of DHCR24 is significantly up-regulated by HCV infection in human hepatocytes.

Role of DHCR24 in HCV replication

Since augmentation of DHCR24 expression was observed by HCV infection in humanized chimeric mice, we next examined whether DHCR24 was involved in HCV replication or not. We transfected siRNA into HCV replicon cell lines FLR3-1 (Fig. 2A and B) and R6FLR-N (Fig. 2C and D). Treatment with either two different *DHCR24* siRNA molecules (siDHCR24-417 or -1024) decreased HCV replication in a dose-dependent manner (Fig. 2A and C) but did not appear to have a significant effect on cell viability (Fig. 2B and D). Western blot analysis using HCV subgenomic replicon cell lines confirmed these findings (Fig. 2E and F). We also transfected the *DHCR24* siRNAs into HCV JFH-1 strain [18]-infected HuH7/K4 cell lines and found, by Western blot analysis, that the siRNAs inhibited HCV protein expression (Fig. 2G and H). These results indicate that DHCR24 may play a role in HCV replication.

The expression level of DHCR24 is linked to intracellular cholesterol levels

Human DHCR24 is involved in cholesterol biosynthesis [10]. It participates in multiple steps of cholesterol synthesis from lanosterol [26] (Fig. 3A). To examine the effect of cholesterol on the DHCR24 expression level in HuH-7 cells, we added cholesterol to cultured cells and determined the DHCR24 expression level (Fig. 3B). Expression levels of DHCR24 in HuH-7 cells were decreased approximately 50% by addition of cholesterol compared to that of the untreated control (Fig. 3B). On the other hand, that of DHCR24 in HepG2 cells was increased 2.5-fold by depletion of cholesterol using methyl-β-cyclodextrin (M-β-CD) (Fig. 3C).

These results indicate that the expression of DHCR24 in a cell correlates with the cholesterol level in that cell. Furthermore, silencing *DHCR24* reduced the cholesterol level in cells compared to control cells (Fig. 3D), suggesting that DHCR24 is essential for cholesterol synthesis.

Effect of U18666A on HCV replication in vitro

We further examined the role that DHCR24 plays in HCV replication by treating cells with U18666A. Treatment with U18666A (62.5, 125, 250, 500, and 1000 nM) of HCV replicon cells (FLR3-1) decreased HCV replication in a dose-dependent manner as shown by luciferase assay (Fig. 4A) and Western blot analysis (Fig. 4B). Notably, DHCR24 protein appeared as doublet bands in the absence of U18666A, but the lower band shifted to the upper band after treatment with U18666A (Fig. 4B). U18666A also suppressed HCV replication in other replicon cell lines (R6FLR-N and Rep JFH Luc 3-13; Fig. 4C and D). Treatment with U18666A (<250 nM) suppressed viral replication without producing significant cytotoxicity. We also examined the effect of 7-dehydrocholesterol reductase (DHCR7) (Fig. 3A) on HCV replication using the specific inhibitor BD1008 [26]. Treatment with BD1008 also suppressed HCV replication, but the concentration required was much higher than that needed in the U18666A assays (Fig. 4E); the concentration also greatly exceeded the intrinsic IC_{50} value for inhibition of σ-receptor binding (47 ± 2 nM) [27]. Therefore, DHCR24 may play a more significant role than DHCR7 in HCV replication. We next evaluated the compensatory effect that the addition of cholesterol had on cells treated with U18666A (Fig. 4F and G) by examining low density lipoprotein (LDL)-replaceable dissolved cholesterol levels as described in Supplementary data. Treatment with cholesterol led to partial restoration of HCV replication (Fig. 4F). These results suggest that U18666A suppresses HCV replication by depleting cellular cholesterol stores.

Next, we characterized the effect that U18666A had on HCV JFH-1 infection. Adding U18666A (62.5, 125, 250, and 500 nM) to HCV JFH-1-infected cell lines for 72 h, reductions of NS5B protein level were observed in cells treated more than 500 nM of U18666A (Fig. 5A and B). Additionally, the HCV RNA copy number in infected cells was suppressed by addition of 250 or 500 nM of U18666A (Fig. 5C). Examination of the cytotoxicity that U18666A (62.5–500 nM) had on infected cells revealed that it had little effect on cell viability (Fig. 5D). These results demonstrate that inhibition of DHCR24 by U18666A suppresses viral replication in HCV replicon cells and HCV-infected cells.

Evaluation of the anti-HCV effect of U18666A in vivo

To examine the effect of U18666A on HCV infection *in vivo*, we administered U18666A to HCV-infected chimeric mice with the humanized liver. The mice were infected with HCV via inoculation of patient serum HCR6 5 weeks after transplantation of human hepatocytes. U18666A (10 mg/kg) and PEG-IFN-α (30 μg/kg) were then administrated to these mice for 2 weeks (Fig. 6A). HCV RNA quantity (Fig. 6B) and serum human albumin levels (Fig. 6C) were measured in the mice after 1, 4, and 14 days of HCV infection. Treatment with U18666A alone significantly decreased HCV RNA levels in the serum (from 1×10^8 to 3×10^5 copies/ml) after 2 weeks, and its suppressive effect was more pronounced than that of PEG-IFN-α alone (8×10^5 copies/ml; Fig. 6B). Moreover, co-administration of U18666A and PEG-IFN-α synergistically (combination index <1) enhanced the antiviral effect of PEG-IFN-α (5×10^4 copies/ml). Treatment with these drugs did not significantly affect the serum human albumin concentrations in treated mice (Fig. 6C).

Discussion

The results of this study revealed that DHCR24, an enzyme that participates in cholesterol synthesis (last step; Fig. 3A), also plays a significant role in HCV replication. To our knowledge, this is the first report that this molecule is involved in HCV infection. The mevalonate route of the cholesterol synthesis pathway (starting from acetyl Co-A) has previously been reported to be involved in

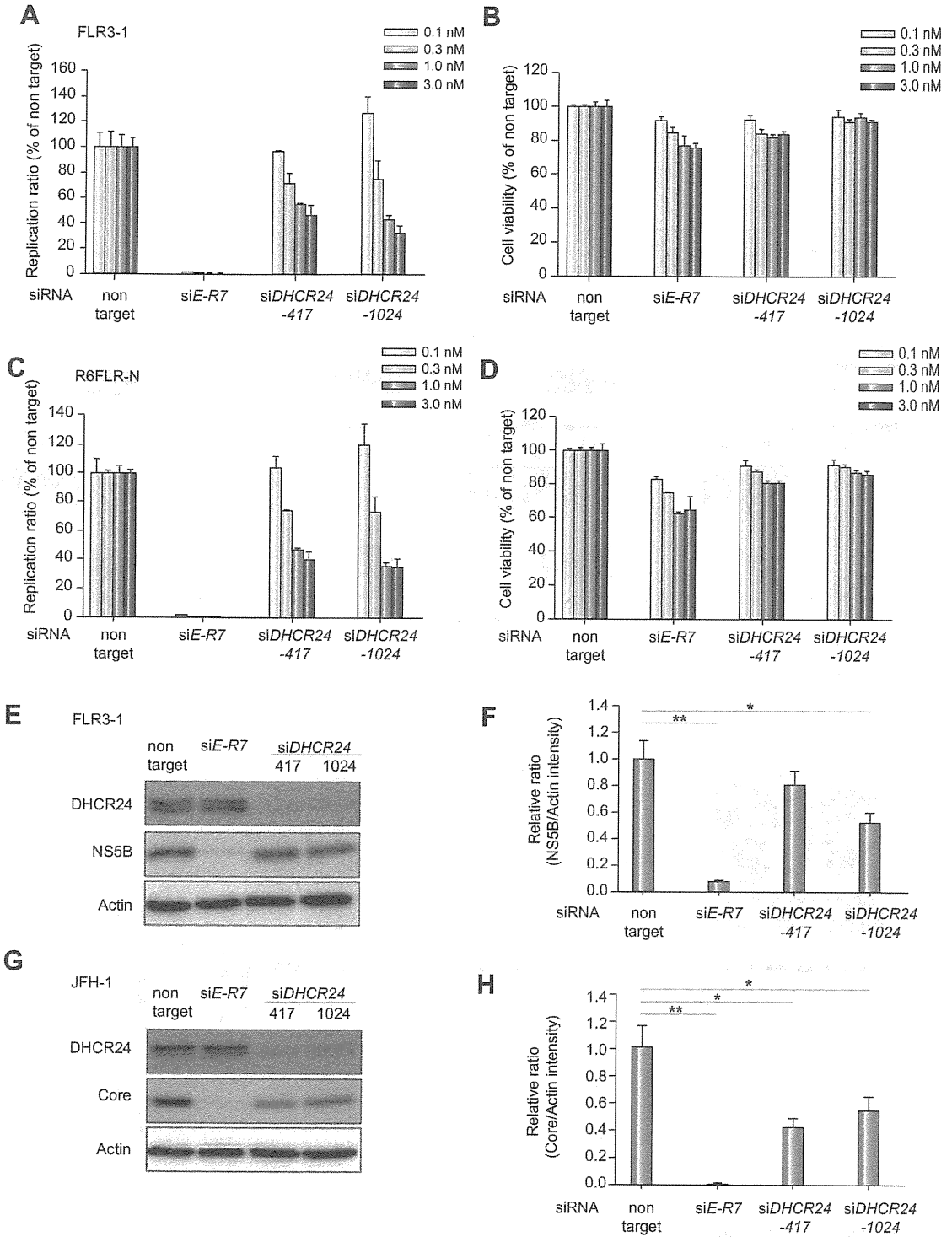

Fig. 2. Effect of DHCR24 knockdown on HCV replication. (A–D) Effect of DHCR24 knockdown on HCV replication in HCV replicon cells (FLR3-1 and R6FLR-N) at 72 h after the anti-*DHCR24* siRNAs (417 and 1024), siRNAs against HCV (siE-R7 for FLR3-1 and JFH-1; siE-R5 for R6-FLR-N), or non-target control siRNAs were transfected into HCV replicon cells. Replication activity was examined by luciferase assay (A and C), and cell viability was measured by the WST-8 assay (B and D). The data represent the mean of three experiments, and the bars indicate SD values. The Western blot analysis (E) and relative intensity of HCV-NS5B protein band was measured by LAS3000 and normalized with that of actin (F) after the treatment with siRNAs targeted against *DHCR24* (siDHCR24-417 and 1024) or HCV (si*E-R7*) in FLR3-1 replicon cells. (G and H) In HCV JFH-1-infected cells, DHCR24 knockdown by si*DHCR*24-417 and 1024 and HCV knockdown by siE-R7 were performed, and DHCR24 and HCV core protein expressions were confirmed by Western blot analysis. The relative intensity ratio of core protein to actin is indicated (H). The data represent the mean of three experiments, and the bars indicate SD values. $^{*}p$ <0.05, $^{**}p$ <0.01 (two-tailed Student's t test).

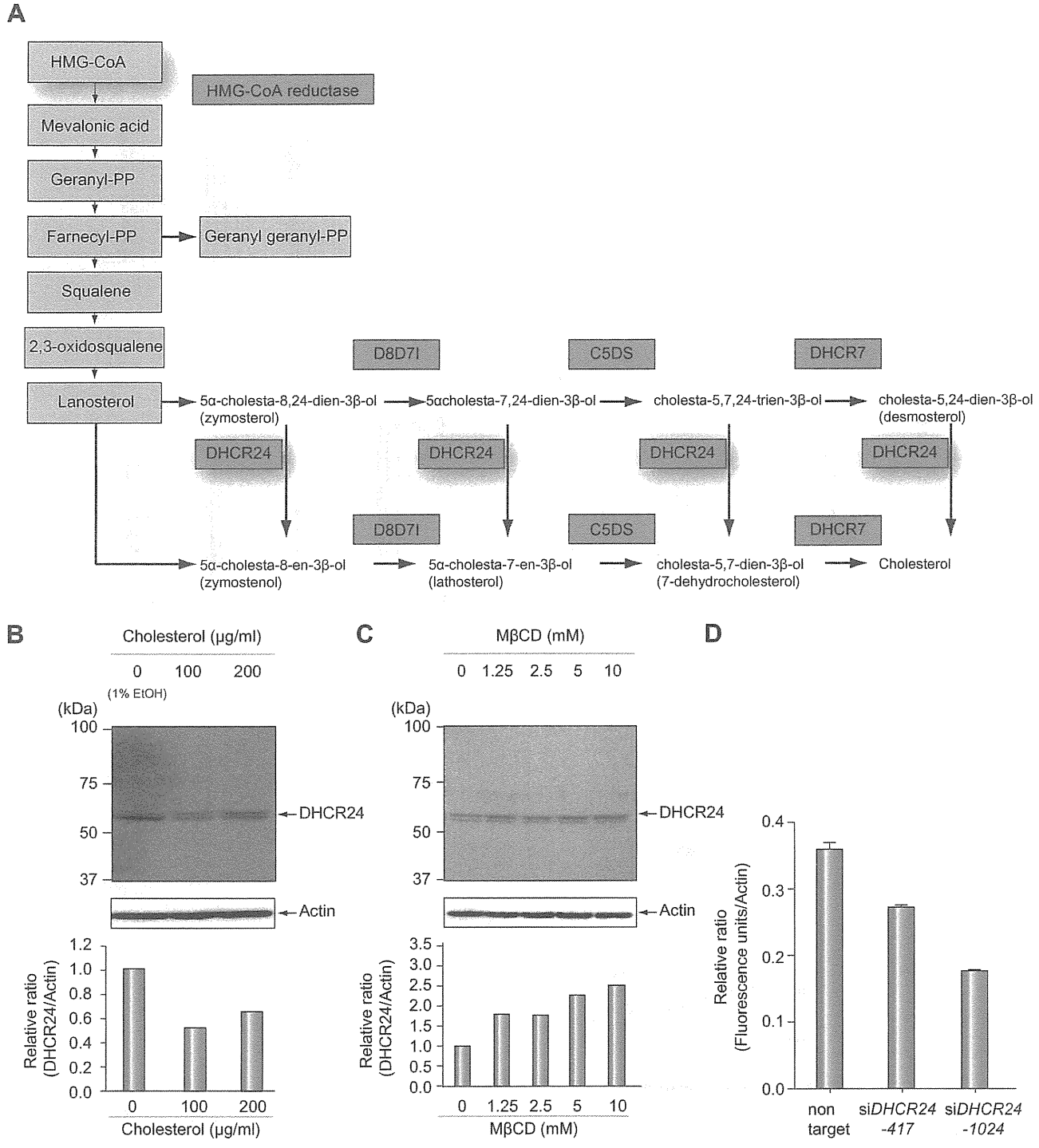

Fig. 3. The level of cholesterol and DHCR24 expression. (A) Cholesterol synthesis pathway, starting from HMG-CoA [26]. The abbreviations used are: D8D7I, 3β-hydroxysterol-delta(8)-delta(7)-isomerase; and C5DS, 3β-hydroxysterol-C^5-desaturase. (B) Cholesterol (0, 100, and 200 μg/ml) was added to HuH-7 cells, and, after 24 h, DHCR24 protein was detected by Western blot analysis using anti-DHCR24 MoAb and protein band intensity was measured and normalized to actin (lower panel). (C) HepG2 cells were treated with MβCD (0, 1.25, 2.5, 5, and 10 mM) for 30 min. After 72 h, these cells were harvested and examined by Western blot analysis with the anti-DHCR24 MoAb and relative intensity was measured as described in (B) (lower panel). (D) Cholesterol concentration in R6FLR-N cells was measured after treatment with non-targeting siRNA and *DHCR24* siRNA (417 and 1024). The cholesterol contents were measured by Amplex Red cholesterol assay, plotted based on fluorescence units and normalized to actin which was measured by Western blot analysis, and the relative ratio was then calculated. The data represent the mean of three experiments, and the bars indicate the SD values.

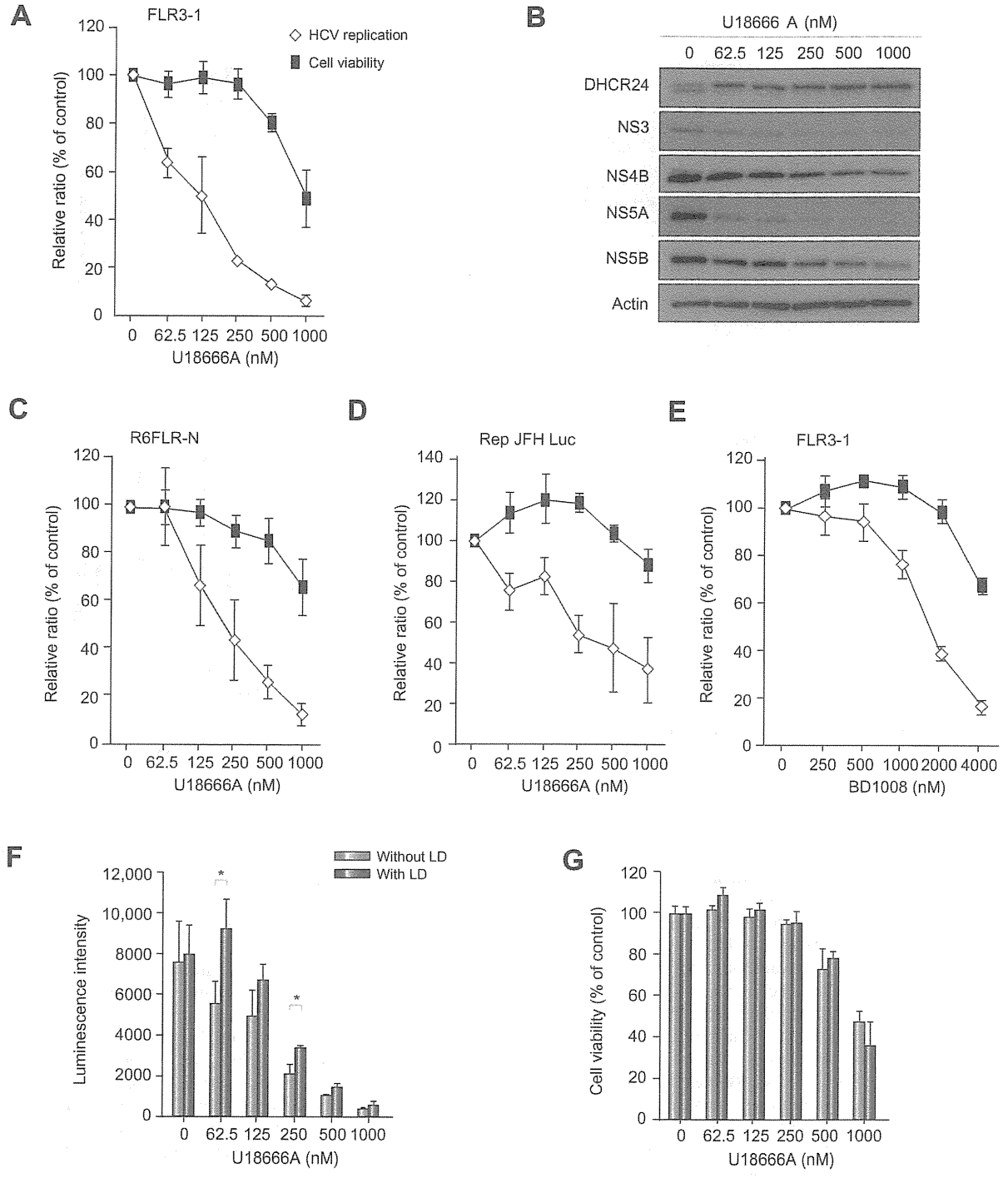

Fig. 4. Effect of U18666A on HCV replication. (A) Addition of U18666A to FLR3-1 cells and subsequent examination of HCV replication by the luciferase assay. Cell viability was measured by WST-8 assay. HCV replication and cell viability were measured 48 h after addition of U18666A. The bars indicate SD values. Open diamonds indicate the relative ratio of viral replication, and black squares indicate the cell viability in relation to untreated controls (A and C–E). (B) Treatment of FLR3-1 cells with U18666A decreased the expression of HCV proteins in a dose-dependent manner, as determined by Western blot analysis. (C and D) Effect of U18666A on HCV replication in other HCV replicon cells (C, R6FLR-N cells; D, Rep JFH Luc 3-13 cells). HCV replication and cell viability analyses were performed as described above. (E) The effect of the DHCR7 inhibitor BD1008 on HCV replicon cells (FLR3-1). Replication activity was examined by the luciferase assay, and cell viability was measured by the WST-8 assay. HCV replication and cell viability analyses were performed 48 h after the addition of U18666A. (F and G) FLR3-1 cells (5×10^3 cells/well) were treated with U18666A alone (light blue, or), low density lipoprotein (LDL) (final cholesterol concentration, 50 μg/ml), and U18666A (dark blue). HCV replication was determined by the luciferase assay 48 h later (F), and cell viability was measured by the WST-8 assay (G). *p <0.05 (two-tailed Student's t-test). The data represent the mean of three experiments, and the bars indicate SD values.

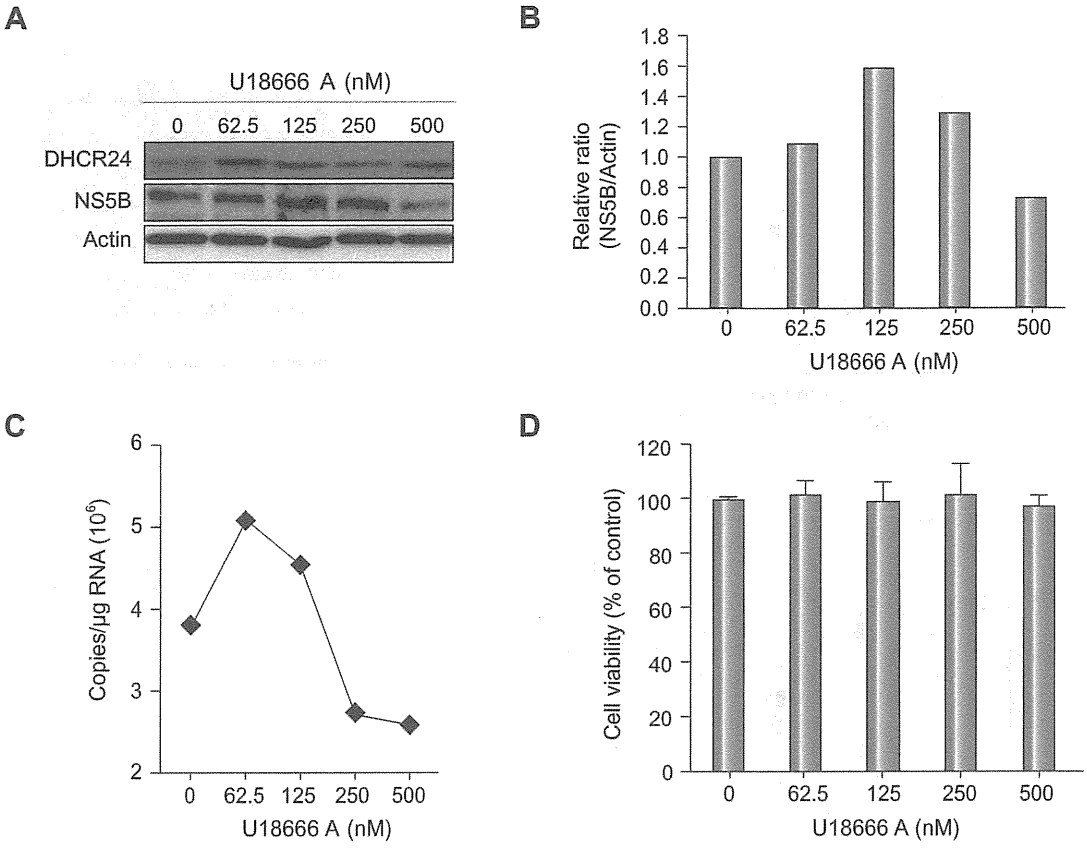

Fig. 5. Effect of U18666A on cells infected with HCV JFH-1. HCV JFH-1-infected cells treated with U18666A were examined 72 h after treatment. (A) Expression of HCV-NS5B protein with or without U18666A treatment, analyzed by Western blot analysis. (B) The intensity of HCV-NS5B protein expression is represented graphically. (C) HCV RNA in HCV JFH-1-infected cells with or without U18666A treatment was measured by RTD-PCR as described in Materials and methods. (D) Cell viability was measured by the WST-8 assay.

HCV replication [28]. The present findings are the first evidence that overexpression of one of the enzymes downstream of the mevalonate pathway, i.e., DHCR24, can be induced by HCV infection. In a previous study, 3-hydroxy 3-methyl-glutaryl Co-A (HMG-CoA) reductase was found to be inhibited by lovastatin, subsequently resulting in suppression of HCV replication [28]. The product of the mevalonate pathway that is required for HCV replication is reported to be a geranyl geranyl lipid [29]. Many lipids are crucial to the viral life cycle, and inhibitors of the cholesterol/fatty acid biosynthetic pathway inhibit viral replication, maturation, and secretion [30,31]. We found that inhibition of DHCR24 down-regulated HCV replication. DHCR24 catalyzes the reduction of the delta-24 bond of the sterol intermediate and works further downstream of farnesyl pyrophosphate (Fig. 3A) and, therefore, does not influence geranyl–geranylation. Thus, our findings indicate the existence of regulatory pathway of HCV replication by cholesterol synthesis and trafficking through DHCR24 rather than by protein geranyl–geranylation. DHCR24 deficiency reduces the cholesterol level and disorganizes cholesterol-rich detergent-resistant membrane domains (DRMs) in mouse brains [32]. Additionally, the HCV replication complex has been detected in the DRM fraction [11]. Therefore, a deficiency in DRM, induced by silencing *DHCR24*, may suppress HCV replication.

We demonstrated that the addition of cholesterol to HCV-infected hepatocytes treated with U18666A led to partial recovery of HCV replication, which suggests that cholesterol may be an important factor in HCV replication. U18666A impairs the intracellular biosynthesis and transport of cholesterol and inhibits the action of membrane-bound enzymes, including DHCR24, during sterol synthesis [33]. Moreover, the DHCR7 inhibitor BD1008 also suppresses HCV replication. Thus, the findings in this study further substantiate the fact that cholesterol plays an important role in HCV replication and infection.

Although monotherapy with statins is reportedly insufficient to induce anti-viral activity in HCV-infected patients [34], a synergistic action between statins and IFN has been observed [35]. The effect of the statin is thought to be mainly mediated by the depletion of geranyl geranyl lipids. It is important to note that higher doses of statins may increase the risk of myopathy, liver dysfunction, and cardiovascular events [36]. Moreover, the EC_{50} values of the statins that are associated with a reduction in HCV replication are reported to be 0.45–2.16 μM, while the IC_{50} of U18666A was estimated to be 125 nM in the present study. Therefore, U18666A may serve as a novel anti-HCV drug that could be utilized with IFN as a combined therapeutic regimen.

In summary, we demonstrated that the expression of DHCR24 is induced by infection with HCV and that DHCR24 is an essential host factor that is required for HCV replication. HCV may increase cholesterol synthesis in cells via the action of a host regulatory factor, such as DHCR24, that is correlated with cholesterol

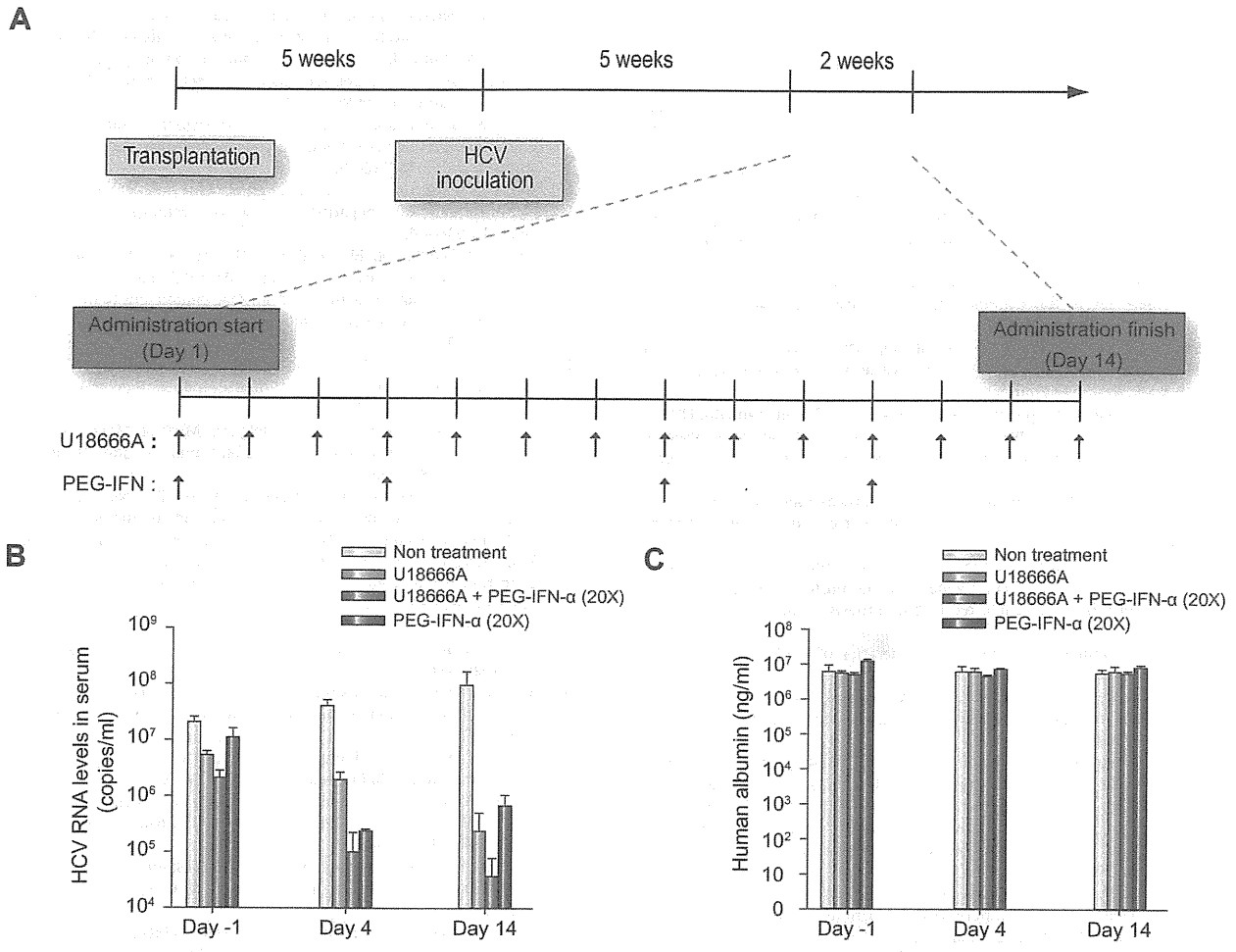

Fig. 6. Evaluation of the anti-HCV effect of U18666A in chimeric mice. (A) Diagram of the schedule that was followed to produce chimeric mice with the humanized liver, perform blood sampling, and administer drugs to chimeric mice infected with HCV. Four groups of three chimeric mice with the humanized liver were treated intraperitoneally with U18666A (10 mg/kg) and/or subcutaneously with PEG-IFN-α (30 μg/kg) at 2-day intervals for 2 weeks. (B) The effect of U18666A and/or PEG-IFN-α on HCV replication in chimeric mice with the humanized liver was determined by quantification of HCV-RNA using RTD-PCR. The bars indicate SD values ($n = 12$). (C) Human albumin concentrations in the sera of chimeric mice with the humanized liver. The bars indicate SD values ($n = 12$).

synthesis and is also directly involved in replication. Genome-wide analysis of the host response to HCV infection revealed the upregulation of genes related to lipid metabolism [37]. DHCR24 expression was found to be upregulated in the cDNA microarray analysis of chronic hepatitis C cases [38]. Future studies are needed to examine the detailed mechanism by which HCV infection augments DHCR24 expression in hepatocytes.

Conflict of interest

The authors who have taken part in this study declared that they do not have anything to disclose regarding funding or conflict of interest with respect to this manuscript.

Financial support

This study was supported in part by a grant from the Ministry of Education, Culture, Sports, Science and Technology of Japan, a grant from the Ministry of Health, Labor and Welfare of Japan, and the Program for Promotion of Fundamental Studies in Health Sciences of the National Institute of Biomedical Innovation of Japan and the Cooperative Research Project on Clinical and Epidemiological Studies of Emerging and Re-emerging Infectious Diseases.

Acknowledgments

We are very grateful to Dr. T. Watanabe, Dr. S. Nakagawa, Mr. T. Nishimura and Dr. K. Tanaka for technical support, and Dr. S. To'ne, Dr. T. Wakita, Dr. S. Sekiguchi, and Dr. F. Yasui for helpful discussions.

Supplementary data

Supplementary data associated with this article can be found, in the online version, at doi:10.1016/j.jhep.2010.12.011.

References

[1] Llovet JM, Burroughs A, Bruix J. Hepatocellular carcinoma. Lancet 2003;362:1907–1917.
[2] Tsukuma H, Hiyama T, Tanaka S, et al. Risk factors for hepatocellular carcinoma among patients with chronic liver disease. N Engl J Med 1993;328:1797–1801.
[3] Wasley A, Alter MJ. Epidemiology of hepatitis C: geographic differences and temporal trends. Semin Liver Dis 2000;20:1–16.
[4] Kohara M, Tanaka T, Tsukiyama-Kohara K, et al. Hepatitis C virus genotypes 1 and 2 respond to interferon-alpha with different virologic kinetics. J Infect Dis 1995;172:934–938.
[5] Tsukiyama-Kohara K, Tone S, Maruyama I, et al. Activation of the CKI-CDK-Rb-E2F pathway in full genome hepatitis C virus-expressing cells. J Biol Chem 2004;279:14531–14541.
[6] Nishimura T, Kohara M, Izumi K, et al. Hepatitis C virus impairs p53 via persistent overexpression of 3beta-hydroxysterol Delta24-reductase. J Biol Chem 2009;284:36442–36452.
[7] Greeve I, Hermans-Borgmeyer I, Brellinger C, et al. The human DIMINUTO/DWARF1 homolog seladin-1 confers resistance to Alzheimer's disease-associated neurodegeneration and oxidative stress. J Neurosci 2000;20:7345–7352.
[8] Wu C, Miloslavskaya I, Demontis S, Maestro R, Galaktionov K. Regulation of cellular response to oncogenic and oxidative stress by Seladin-1. Nature 2004;432:640–645.
[9] Waterham HR, Koster J, Romeijn GJ, et al. Mutations in the 3beta-hydroxysterol Delta24-reductase gene cause desmosterolosis, an autosomal recessive disorder of cholesterol biosynthesis. Am J Hum Genet 2001;69:685–694.
[10] Wechsler A, Brafman A, Shafir M, et al. Generation of viable cholesterol-free mice. Science 2003;302:2087.
[11] Aizaki H, Lee KJ, Sung VM, Ishiko H, Lai MM. Characterization of the hepatitis C virus RNA replication complex associated with lipid rafts. Virology 2004;324:450–461.
[12] Di Stasi D, Vallacchi V, Campi V, et al. DHCR24 gene expression is upregulated in melanoma metastases and associated to resistance to oxidative stress-induced apoptosis. Int J Cancer 2005;115:224–230.
[13] Bierkamper GG, Cenedella RJ. Induction of chronic epileptiform activity in the rat by an inhibitor of cholesterol synthesis, U18666A. Brain Res 1978;150:343–351.
[14] Nakabayashi H, Taketa K, Miyano K, Yamane T, Sato J. Growth of human hepatoma cells lines with differentiated functions in chemically defined medium. Cancer Res 1982;42:3858–3863.
[15] Knowles BB, Howe CC, Aden DP. Human hepatocellular carcinoma cell lines secrete the major plasma proteins and hepatitis B surface antigen. Science (New York, NY) 1980;209:497–499.
[16] Sakamoto H, Okamoto K, Aoki M, et al. Host sphingolipid biosynthesis as a target for hepatitis C virus therapy. Nat Chem Biol 2005;1:333–337.
[17] Watanabe T, Sudoh M, Miyagishi M, et al. Intracellular-diced dsRNA has enhanced efficacy for silencing HCV RNA and overcomes variation in the viral genotype. Gene Ther 2006;13:883–892.
[18] Wakita T, Pietschmann T, Kato T, et al. Production of infectious hepatitis C virus in tissue culture from a cloned viral genome. Nat Med 2005;11:791–796.
[19] Inoue K, Umehara T, Ruegg UT, et al. Evaluation of a cyclophilin inhibitor in hepatitis C virus-infected chimeric mice in vivo. Hepatology 2007;45:921–928.
[20] Jensen ON, Wilm M, Shevchenko A, Mann M. Sample preparation methods for mass spectrometric peptide mapping directly from 2-DE gels. Methods Mol Biol (Clifton, NJ) 1999;112:513–530.
[21] Nakagawa S, Umehara T, Matsuda C, et al. Hsp90 inhibitors suppress HCV replication in replicon cells and humanized liver mice. Biochem Biophys Res Commun 2007;353:882–888.
[22] Takeuchi T, Katsume A, Tanaka T, et al. Real-time detection system for quantification of hepatitis C virus genome. Gastroenterology 1999;116:636–642.
[23] Mercer DF, Schiller DE, Elliott JF, et al. Hepatitis C virus replication in mice with chimeric human livers. Nat Med 2001;7:927–933.
[24] Tateno C, Yoshizane Y, Saito N, et al. Near completely humanized liver in mice shows human-type metabolic responses to drugs. Am J Pathol 2004;165:901–912.
[25] Umehara T, Sudoh M, Yasui F, et al. Serine palmitoyltransferase inhibitor suppresses HCV replication in a mouse model. Biochem Biophys Res Commun 2006;346:67–73.
[26] Kedjouar B, de Medina P, Oulad-Abdelghani M, et al. Molecular characterization of the microsomal tamoxifen binding site. J Biol Chem 2004;279:34048–34061.
[27] John CS, Lim BB, Geyer BC, Vilner BJ, Bowen WD. 99mTc-labeled sigma-receptor-binding complex: synthesis, characterization, and specific binding to human ductal breast carcinoma (T47D) cells. Bioconjug Chem 1997;8:304–309.
[28] Ye J, Wang C, Sumpter Jr R, et al. Disruption of hepatitis C virus RNA replication through inhibition of host protein geranyl-geranylation. Proc Natl Acad Sci USA 2003;100:15865–15870.
[29] Kapadia SB, Chisari FV. Hepatitis C virus RNA replication is regulated by host geranyl-geranylation and fatty acids. Proc Natl Acad Sci USA 2005;102:2561–2566.
[30] Aizaki H, Morikawa K, Fukasawa M, et al. Critical role of virion-associated cholesterol and sphingolipid in hepatitis C virus infection. J Virol 2008;82:5715–5724.
[31] Syed GH, Amako Y, Siddiqui A. Hepatitis C virus hijacks host lipid metabolism. Trends Endocrinol Metab 2010;21:33–40.
[32] Crameri A, Biondi E, Kuehnle K, et al. The role of seladin-1/DHCR24 in cholesterol biosynthesis, APP processing and Abeta generation in vivo. EMBO J 2006;25:432–443.
[33] Cenedella RJ. Cholesterol synthesis inhibitor U18666A and the role of sterol metabolism and trafficking in numerous pathophysiological processes. Lipids 2009;44:477–487.
[34] Bader T, Fazili J, Madhoun M, et al. Fluvastatin inhibits hepatitis C replication in humans. Am J Gastroenterol 2008;103:1383–1389.
[35] Ikeda M, Abe K, Yamada M, et al. Different anti-HCV profiles of statins and their potential for combination therapy with interferon. Hepatology (Baltimore, MD) 2006;44:117–125.
[36] Argo CK, Loria P, Caldwell SH, Lonardo A. Statins in liver disease: a molehill, an iceberg, or neither? Hepatology (Baltimore, MD) 2008;48:662–669.
[37] Su AI, Pezacki JP, Wodicka L, et al. Genomic analysis of the host response to hepatitis C virus infection. Proc Natl Acad Sci USA 2002;99:15669–15674.
[38] Honda M, Yamashita T, Ueda T, et al. Different signaling pathways in the livers of patients with chronic hepatitis B or chronic hepatitis C. Hepatology 2006;44:1122–1138.

Persistent expression of the full genome of hepatitis C virus in B cells induces spontaneous development of B-cell lymphomas in vivo

*Yuri Kasama,[1] *Satoshi Sekiguchi,[2] Makoto Saito,[1] Kousuke Tanaka,[1] Masaaki Satoh,[1] Kazuhiko Kuwahara,[3] Nobuo Sakaguchi,[3] Motohiro Takeya,[4] Yoichi Hiasa,[5] Michinori Kohara,[2] and Kyoko Tsukiyama-Kohara[1]

[1]Department of Experimental Phylaxiology, Faculty of Life Sciences, Kumamoto University, Kumamoto, Japan; [2]Department of Microbiology and Cell Biology, Tokyo Metropolitan Institute of Medical Science, Tokyo, Japan; [3]Department of Immunology, Faculty of Life Sciences, Kumamoto University, Kumamoto, Japan; [4]Department of Cell Pathology, Faculty of Life Sciences, Kumamoto University, Kumamoto, Japan; and [5]Department of Gastroenterology and Metabology, Ehime University Graduate School of Medicine, To-on, Ehime, Japan

Extrahepatic manifestations of hepatitis C virus (HCV) infection occur in 40%-70% of HCV-infected patients. B-cell non-Hodgkin lymphoma is a typical extrahepatic manifestation frequently associated with HCV infection. The mechanism by which HCV infection of B cells leads to lymphoma remains unclear. Here we established HCV transgenic mice that express the full HCV genome in B cells (RzCD19Cre mice) and observed a 25.0% incidence of diffuse large B-cell non-Hodgkin lymphomas (22.2% in males and 29.6% in females) within 600 days after birth. Expression levels of aspartate aminotransferase and alanine aminotransferase, as well as 32 different cytokines, chemokines and growth factors, were examined. The incidence of B-cell lymphoma was significantly correlated with only the level of soluble interleukin-2 receptor α subunit (sIL-2Rα) in RzCD19Cre mouse serum. All RzCD19Cre mice with substantially elevated serum sIL-2Rα levels (> 1000 pg/mL) developed B-cell lymphomas. Moreover, compared with tissues from control animals, the B-cell lymphoma tissues of RzCD19Cre mice expressed significantly higher levels of IL-2Rα. We show that the expression of HCV in B cells promotes non-Hodgkin–type diffuse B-cell lymphoma, and therefore, the RzCD19Cre mouse is a powerful model to study the mechanisms related to the development of HCV-associated B-cell lymphoma. (*Blood*. 2010;116(23):4926-4933)

Introduction

More than 175 million people worldwide are infected with hepatitis C virus (HCV), a positive-strand RNA virus that infects both hepatocytes and peripheral blood mononuclear cells.[1] Chronic HCV infection may lead to hepatitis, liver cirrhosis, hepatocellular carcinomas[2,3] and lymphoproliferative diseases such as B-cell non-Hodgkin lymphoma and mixed-cryoglobulinemia.[1,4-6] B-cell non-Hodgkin lymphoma is a typical extrahepatic manifestation frequently associated with HCV infection[7] with geographic and ethnic variability.[8,9] Based on a meta-analysis, the prevalence of HCV infection in patients with B-cell non-Hodgkin lymphoma is approximately 15%.[8] The HCV envelope protein E2 binds human CD81,[10] a tetraspanin expressed on various cell types including lymphocytes, and activates B-cell proliferation[11]; however, the precise mechanism of disease onset remains unclear. We previously developed a transgenic mouse model that conditionally expresses HCV cDNA (nucleotides 294-3435), including the viral genes that encode the core, E1, E2, and NS2 proteins, using the Cre/*lox*P system (in core~NS2 [CN2] mice).[12,13] The conditional transgene activation of the HCV cDNA (core, E1, E2, and NS2) protects mice from Fas-mediated lethal acute liver failure by inhibiting cytochrome c release from mitochondria.[13] In HCV-infected mice, persistent HCV protein expression is established by targeted disruption of *irf-1*, and high incidences of lymphoproliferative disorders are found in CN2 *irf-1*$^{-/-}$ mice.[14] Infection and replication of HCV also occur in B cells,[15,16] although the direct effects, particularly in vivo, of HCV infection on B cells have not been clarified.

To define the direct effect of HCV infection on B cells in vivo, we crossed transgenic mice with an integrated full-length HCV genome (Rz) under the conditional Cre/*lox*P expression system with mice expressing the Cre enzyme under transcriptional control of the B lineage–restricted gene *CD19*,[17] we addressed the effects of HCV transgene expression in this study.

Methods

Animal experiments

Wild-type (WT), Rz, CD19Cre, RzCD19Cre mice (129/sv, BALB/c, and C57BL/6J mixed background), and MxCre/CN2-29 mice (C57BL/6J background) were maintained in conventional animal housing under specific pathogen-free conditions. All animal experiments were performed according to the guidelines of the Tokyo Metropolitan Institute of Medical Science or the Kumamoto University Subcommittee for Laboratory Animal Care. The protocol was approved by the Institutional Review Boards of both facilities.

Measurements of HCV protein and RNA

Mice were anesthetized and bled, and tissues (spleen, lymph nodes, liver, and tumors) were homogenized in lysis buffer (1% sodium dodecyl sulfate; 0.5% (wt/vol) nonyl phenoxypolyethoxylethanol; 0.15M NaCl; 10 mM

Submitted May 2, 2010; accepted August 13, 2010. Prepublished online as *Blood* First Edition paper, August 23, 2010; DOI 10.1182/blood-2010-05-283358.

*Y.K. and S.S. contributed equally to this work.

The online version of this article contains a data supplement.

The publication costs of this article were defrayed in part by page charge payment. Therefore, and solely to indicate this fact, this article is hereby marked "advertisement" in accordance with 18 USC section 1734.

tris(hydroxymethyl)aminomethane, pH 7.4) using a Dounce homogenizer. The concentration of HCV core protein in tissue lysates was measured using an HCV antigen enzyme-linked immunosorbent assay (ELISA; Ortho).[18] HCV mRNA was isolated by a guanidine thiocyanate protocol using ISOGEN (Nippon Gene) and was detected by reverse transcription polymerase chain reaction (RT-PCR) amplification using primers specific for the 5′ untranslated region of the *HCR6* sequence.[19,20] Reverse transcription was performed using Superscript III reverse transcriptase (Invitrogen) with random primers. PCR primers NCR-F (5′-TTCACGCAGAAAGCGTCTAGCCAT-3′) and NCR-R (5′-TCGTCCTGGCAATTCCGGTGTACT-3′) were used for the first round of HCV cDNA amplification, and the resulting product was used as a template for a second round of amplification using primers NCR-F INNER (5′-TTCCGCAGACCACTATGGCT-3′) and NCR-R INNER (5′-TTCCGCAGACCACTATGGCT-3′).

Collection of serum for chemokine ELISA

Blood samples were collected from the supraorbital veins or by heart puncture of killed mice. Blood samples were centrifuged at 10 000*g* for 15 minutes at 4°C to isolate the serum.[21] Serum concentrations of interleukin (IL)–1α, IL-1β, IL-2, IL-3, IL-4, IL-5, IL-6, IL-9, IL-10, IL-12(p40), IL-12(p70), IL-13, IL-17, Eotaxin, granulocyte colony-stimulating factor (CSF), granulocyte–macrophage–CSF, interferon (IFN)–γ, keratinocyte-derived chemokine (KC), monocyte chemotactic protein-1, macrophage inflammatory protein (MIP)–1α, MIP-1β, Regulated upon Activation, Normal T-cell Expressed, and Secreted, tumor necrosis factor-α, IL-15, fibroblast growth factor-basic, leukemia inhibitory factor, macrophage-CSF, human monokine induced by gamma interferon, MIP-2, platelet-derived growth factorβ, and vascular endothelial growth factor were measured using the Bio-Plex Pro assay (Bio-Rad). Serum soluble IL-2 receptor α (sIL-2Rα) concentrations were determined by ELISA (DuoSet ELISA Development System; R&D Systems). Serum aspartate aminotransferase (AST) and alanine aminotransferase (ALT) activities were determined using a commercially available kit (Transaminase CII test; Wako Pure Chemical Industries).

Histology and immunohistochemical staining

Mouse tissues were fixed with 4% formaldehyde (Mildform 10 N; Wako Pure Chemical Industries), dehydrated with an ethanol series, embedded in paraffin, sectioned (10-μm thick) and stained with hematoxylin and eosin. For tissue immunostaining, paraffin was removed from the sections using xylene following the standard method,[14] and sections were incubated with anti-CD3 or anti-CD45R (Santa Cruz Biotechnology) in phosphate-buffered saline without Ca^{2+} and Mg^{2+} (pH 7.4) but with 5% skim milk. Next, the sections were incubated with biotinylated anti-rat immunoglobulin (Ig)G (1:500), followed by incubation with horseradish peroxidase-conjugated avidin-biotin complex (Dako Corp), and the color reaction was developed using 3,3′-diaminobenzidine. Sections were observed under an optical microscope (Carl Zeiss).

Detection of immunoglobulin gene rearrangements by PCR

Genomic DNA was isolated from tumor tissues, and PCR was performed as described.[22] In brief, PCR reaction conditions were 98°C for 3 minutes; 30 cycles at 98°C for 30 seconds, 60°C for 30 seconds, 72°C for 1.5 minutes, and 72°C for 10 minutes. Mouse Vk genes were amplified using previously described primers.[23] Amplification of mouse Vj genes was performed using Vκcon (5′-GGCTGCAGSTTCAGTGGCAGTGGRTCWGGRAC-3′; R, purine; W, A or T) and Jκ5 (5′-TGCCACGTCAACTGATAATGAGCCCTCTC-3′) as described.[24]

Results

Establishment of transgenic mice with B lineage–restricted HCV gene expression

We defined the direct effect of HCV infection on B cells in vivo by crossing transgenic mice that had an integrated full-length HCV genome (Rz) under the conditional Cre/*lox*P expression system (Figure 1A upper schematic)[12,19,25] with mice that expressed the Cre enzyme under transcriptional control of the B lineage–restricted gene *CD19*[17] (RzCD19Cre; Figure 1A lower schematic). Expression of the HCV transgene in RzCD19Cre mice was confirmed by ELISA (Figure 1B); a substantial level of HCV core protein was detected in the spleen (370.9 ± 10.2 pg/mg total protein), but levels were lower in the liver (0.32 ± 0.03 pg/mg) and plasma (not detectable). RT-PCR analysis of peripheral blood lymphocytes (PBLs) from RzCD19Cre mice indicated the presence of HCV transcripts (Figure 1C). The weights of RzCD19Cre, Rz (with the full HCV genome transgene alone), CD19Cre (with the Cre gene knock-in at the CD19 gene locus) and WT mice were measured weekly for more than 600 days post birth; there were no significant differences between these groups (data not shown; the total number of transgenic and WT mice was approximately 200). The survival rate in each group was also measured for > 600 days (Figure 1D); survival in the female RzCD19Cre group was lower than that of the other groups.

The spontaneous development of B-cell lymphomas in the RzCD19Cre mouse

At 600 days post birth, mice (n = 140) were killed by bleeding under anesthesia, and tissues (spleen, lymph node, liver, and tumors) were excised and examined by hematoxylin and eosin staining (Figure 2A; supplemental Figure 1, available on the *Blood* Web site; see the Supplemental Materials link at the top of the online article). The incidence of B-cell lymphoma in RzCD19Cre mice was 25.0% (22.2% in males and 29.6% in females) and was significantly higher than the incidence in the HCV-negative groups (Table 1). This incidence is significantly higher than those of the other cell-type tumors developed spontaneously in all mouse groups (supplemental Table 1). Because nodular proliferation of CD45R-positive atypical lymphocytes was observed, lymphomas were diagnosed as typical diffuse B-cell non-Hodgkin lymphomas (Figure 2Aiv,vi-vii; supplemental Figure 1B,E,H,M). Mitotic cells were also positive for CD45R (Figure 2Avi arrowheads). CD3-positive T-lymphocytes were small and had a scattered distribution. Intrahepatic lymphomas had the same immunophenotypic characteristics as B-cell lymphomas (supplemental Figure 1K arrowheads, inset; 1L–N, ID No. 24-4, RzCD19Cre mouse); lymphoma tissues were markedly different compared with the control lymph node (Figure 2Ai,iii,v; ID No. 47-4, CD19Cre mouse) and liver (supplemental Figure 1J; ID No. 24-2, Rz mouse; tissues were from a littermate of the mice used to generate the data in supplemental Figure 1D-I,K-N). All samples were reviewed by at least 2 expert pathologists and classified according to World Health Organization classification.[26] Lymphomas were mostly CD45R positive and located in the mesenteric lymph nodes (Figure 2A; supplemental Figure 1), and some were identified as intrahepatic lymphomas (incidence, 4.2%; supplemental Figure 1K-N). HCV gene expression was detected in all B-cell lymphomas of RzCD19Cre mice (Figure 2B).

To examine the Ig gene configuration in the B-cell lymphomas of the RzCD19Cre mice, genomic DNA was isolated and analyzed by PCR. Ig gene rearrangements were identified in each case (Figure 2C). Genomic DNA isolated from the tumors of a germinal center–associated nuclear protein (GANP) transgenic mouse (GANP Tg#3) yielded a predominant Jk5 PCR product (Figure 2C, Vκ-Jκ); a predominant JH1 product and a minor JH2 product (supplemental Figure 2, DH-JH) were also identified, as previously reported,[22] indicating that the lymphoma cells proliferated from the transformation of an oligo B-cell clone. The B-cell lymphomas of

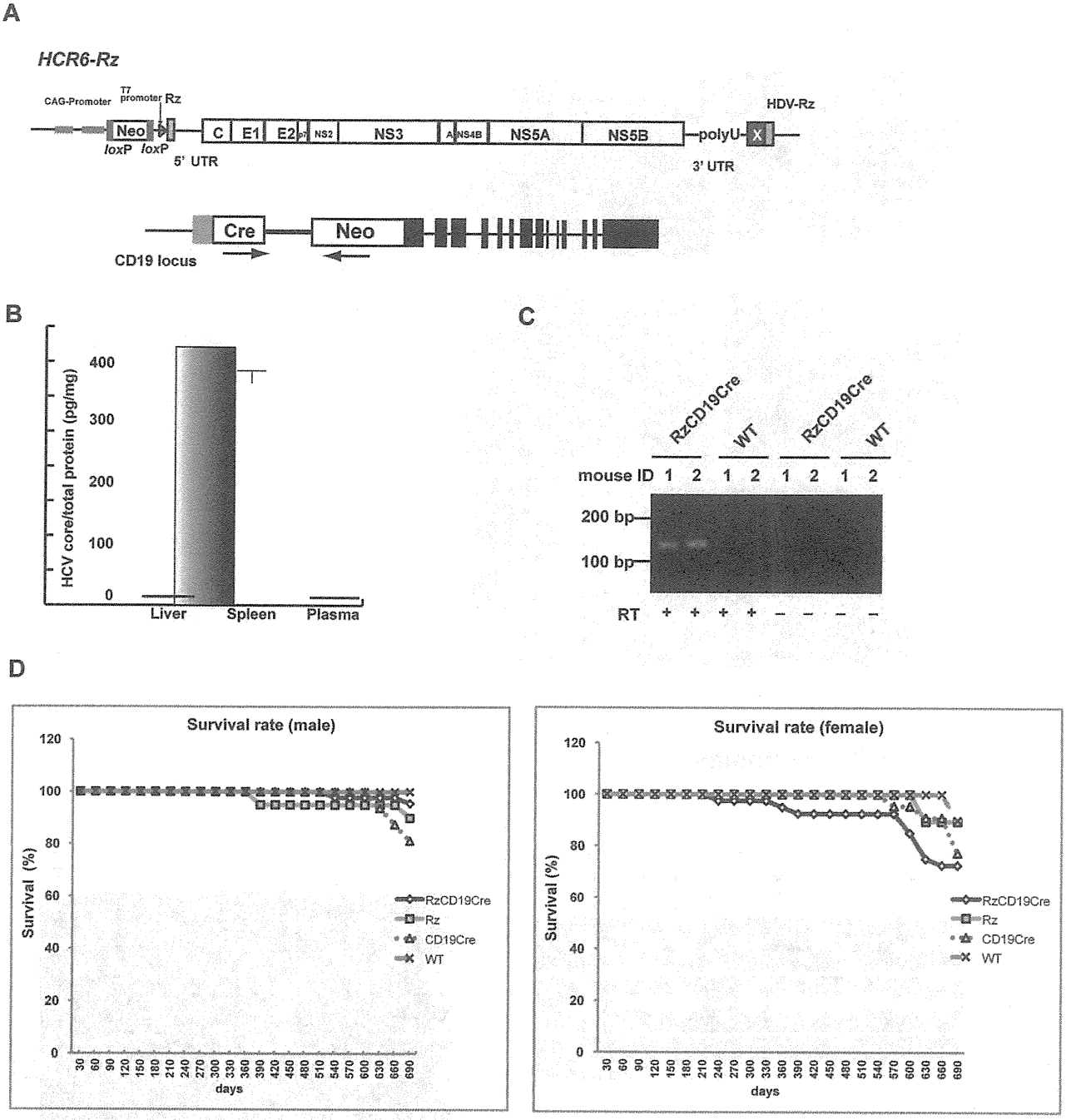

Figure 1. Establishment of RzCD19Cre mice. (A) Schematic diagram of the transgene structure comprising the complete HCV genome (*HCR6-Rz*). HCV genome expression was regulated by the Cre/*loxP* expression cassette (top diagram). The Cre transgene was located in the CD19 locus (bottom diagram). (B) Expression of HCV core protein in the liver, spleen, and plasma of RzCD19Cre mice was quantified by core ELISA. Data represent the mean ± SD (n = 3). (C) Detection of HCV RNA in PBLs by RT-PCR. Samples that included the RT reaction are indicated by +, and those that did not include the RT reaction are indicated by –. (D) Survival rates of male and female RzCD19Cre mice (males, n = 45; females, n = 40), Rz mice (males, n = 20; females, n = 19), CD19Cre mice (males, n = 16; females, n = 22), and WT mice (males, n = 5; females, n = 10).

8 RzCD19Cre mice (mouse ID Nos. 24-1, 54-1, 56-5, 69-5, 42-4, 43-4, 36-3 [data not shown] and 62-2 [data not shown]) yielded a Jκ-5 gene amplification product, and the lymphomas from 3 other mice had the alternative gene configurations Jκ-1 (mouse ID No. 31-4), Jκ-2 (mouse ID No. 24-4) and Jκ-3 (mouse ID No. 42-4; Figure 2C). PCR amplification products from the genes JH4 (mouse ID Nos. 24-1, 24-4, 54-1, 43-4, 56-5, 69-5, 62-2 [data not shown], 36-3 [data not shown]), JH1 (mouse ID Nos. 31-4, 42-4) and JH3 (mouse ID Nos. 31-4, 42-4, 56-5, 43-4, 36-3 [data not shown]) were also detected (supplemental Figure 2). The mutation frequencies in the Jκ-1, -3 and -5 genes were the same as the mutation frequency in the genomic V-region gene.[22] Few or no sequence differences in the variable region were identified among clones from which DNA was amplified. These results indicate the possibility that tumors judged as B-cell lymphomas based on pathology criteria were derived from the transformation of a single germinal center of B-cell origin.

To rule out the oncogenic effect caused by a transgenic integration into a specific genomic locus, we examined if HCV transgene inserted into another genomic site also causes B-cell lymphomas using another HCV transgenic mouse strain, MxCre/CN2-29 (supplemental Figure 3). Expression of the HCV CN2

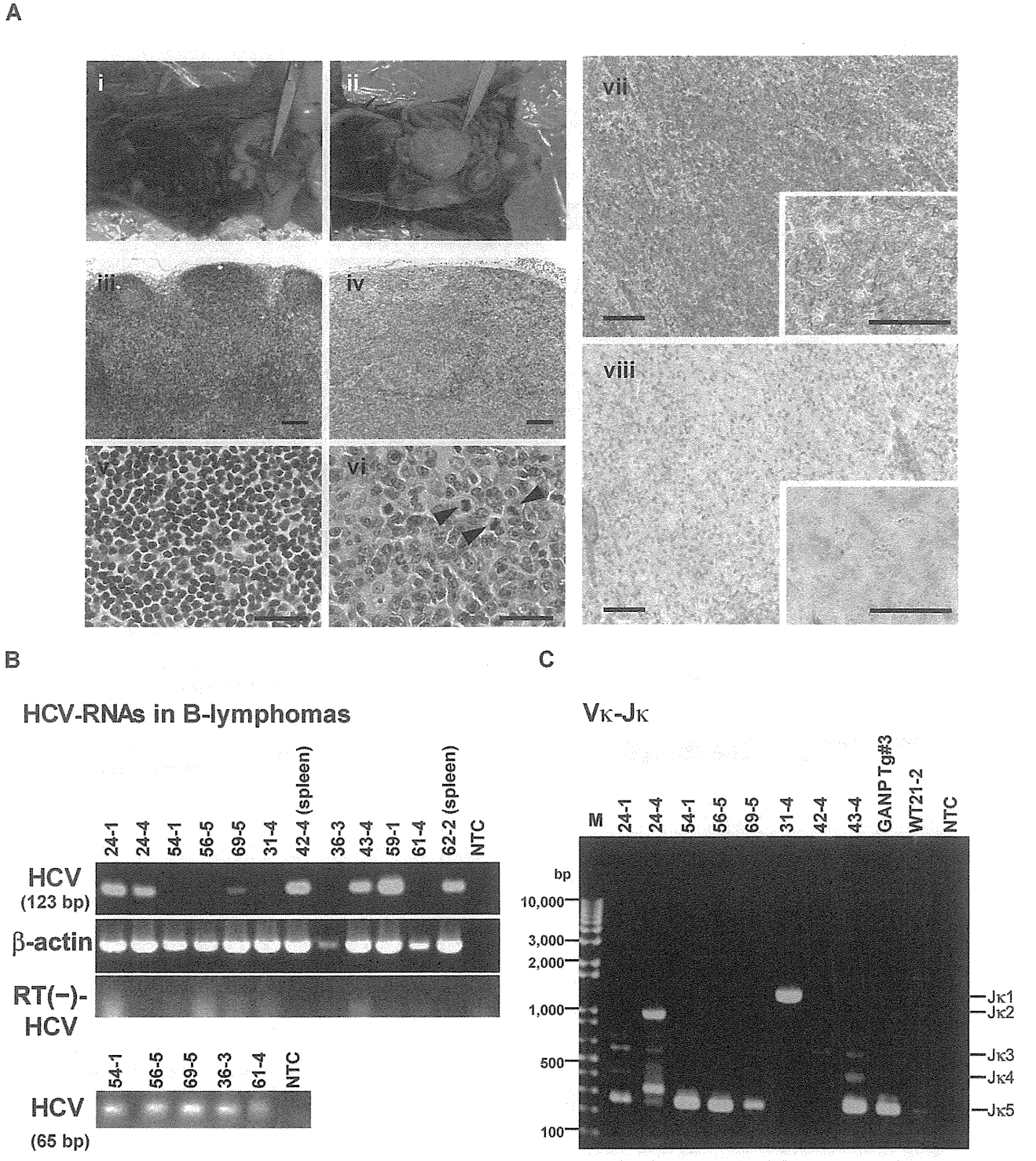

Figure 2. Histopathologic analysis of B-cell lymphomas in RzCD19Cre mouse tissues. (A) Histologic analysis of tissues from a normal mouse (i, iii, v; CD19Cre mouse, ID No. 47-4, male) and a B-cell lymphoma from a RzCD19Cre mouse (ii, iv, vi; ID No. 69-5, male). Paraformaldehyde-fixed and paraffin-embedded tumor tissues were stained with hematoxylin and eosin (iii-vi) or immunostained using anti-CD45R (vii; bottom right, inset) and anti-CD3 (viii; bottom right, inset). Also shown is a macroscopic view of the lymphoma from a mesenchymal lymph node (ii, indicated by forceps), which is not visible in the normal mouse (i). Mitotic cells are indicated with arrowheads (vi). Scale bars: 100 μm (iii-iv, vii-viii) and 20 μm (v-vi, insets in vii-viii). (B) Expression of HCV RNA in B-cell lymphomas from RzCD19Cre mice was examined by RT-PCR. The first round of PCR amplification yielded a 123-base pair fragment of HCV cDNA (upper panel), and a second round of PCR amplification yielded a 65-base pair fragment (lower panel). The β-actin mRNA was a control. As an additional control, the first and second rounds of amplification were performed using samples that had not been subjected to reverse transcription. NTC, no-template control. (C) Ig gene rearrangements in the tumors of RzCD19Cre mice. Genomic DNA isolated from B-cell lymphoma tissues of RzCD19Cre mice (ID Nos. 24-1, 24-4, 54-1, 56-5, 69-5, 31-4, 42-4, 43-4) and spleen tissues of a WT mouse (ID No. 21-2) was PCR amplified using primers specific for Vκ-Jκ genes. Amplification of controls was performed using genomic DNA isolated from a GANP transgenic mouse (GANP Tg#3) and in the absence of template DNA (no-template control, NTC). M, DNA ladder marker.

gene (nucleotides 294-3435)[12] was induced by the Mx promoter-driven cre recombinase with poly(I:C) induction[14] (supplemental Figure 3A). HCV core proteins were detected in both normal spleen (mouse ID Nos. 2, 3, 4) and intra-splenic B-cell lymphoma tissues

Table 1. Lymphoma incidence in HCV-expressing and control mice

HCV expression	Mouse genotype	No.	Incident B lymphoma, number (%)	Incident T lymphoma, number (%)
+	RzCD19Cre	72	18 (25.0)	3 (4.1)
−	Rz	34	1 (2.9)	1 (2.9)
−	CD19Cre	22	2 (9.1)	1 (4.5)
−	WT	12	1 (8.3)	1 (8.3)

(mouse ID Nos. 5, 6, 7) of MxCre/CN2-29 mice but not in spleens of the CN2-29 mouse (mouse ID No. 1, Figure 3B). After 12 months, the MxCre/CN2-29 mice developed B-cell lymphomas in the spleen at a high incidence (33.3%: 3/9), whereas the CN2-29 mice did not (0/13; supplemental Figure 3C), indicating that the development of B-cell lymphomas in HCV transgenic mice occurred similarly to RzCD19Cre mice. MxCre/CN2-29 mice also developed hepatocellular carcinomas (10%, 360 days, 17%, 480 days, 50%, 600 days after onset of HCV expression; Sekiguchi et al, submitted).

The results obtained in 2 HCV transgenic mouse strains indicate that the expression of the HCV gene or the proteins indeed induces the spontaneous development of B-cell lymphomas irrespective of the integrated site in the mouse genome.

The levels of cytokines and chemokines in B-cell lymphomas and other tumors and in tumor-free control mice

Abnormal induction of cytokine production occurs in HCV-associated non-Hodgkin lymphomas[27,28] and in patients with

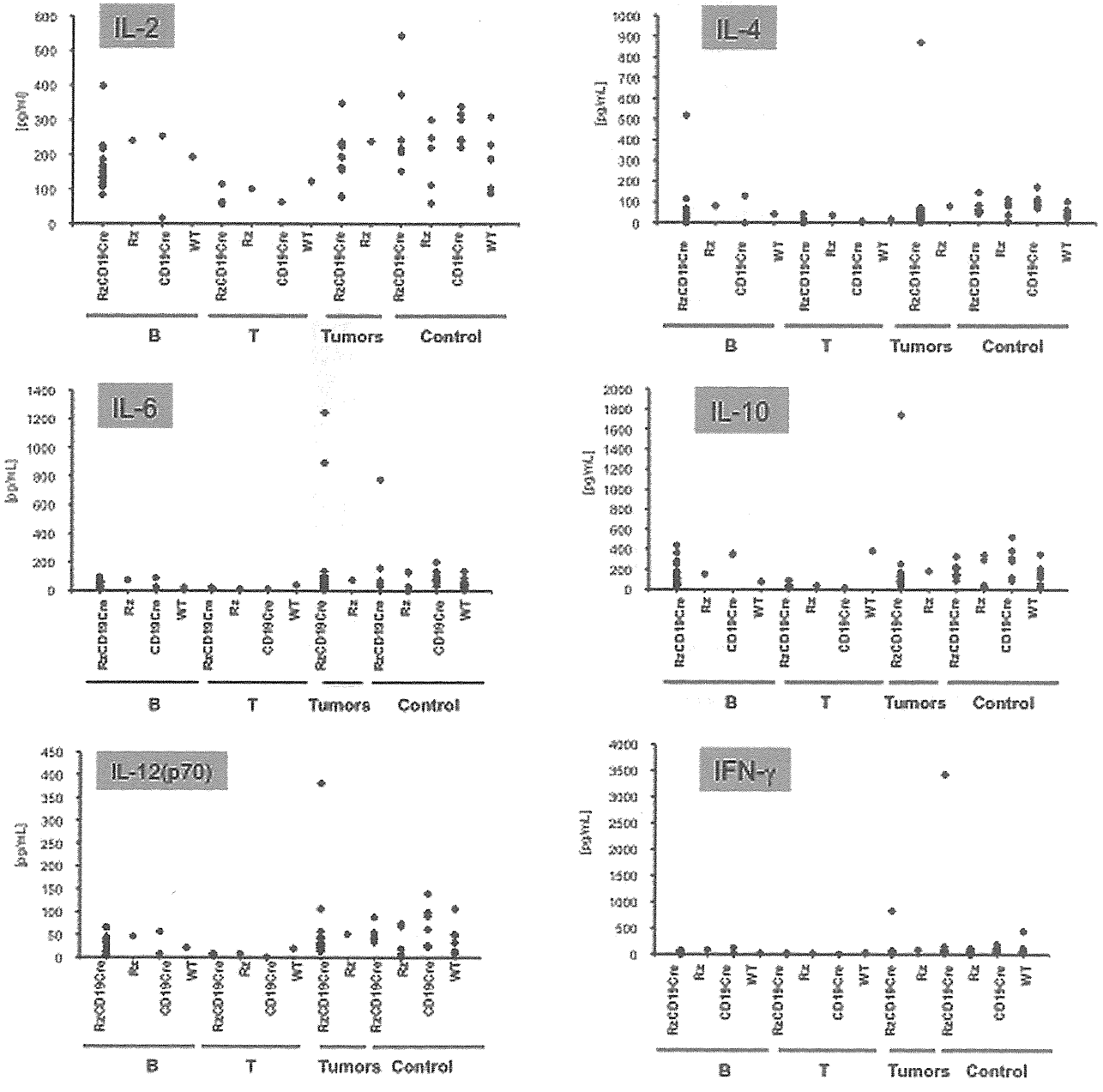

Figure 3. Analysis of serum cytokine levels using a multisuspension array system. The serum concentration levels of IL-2, IL-4, IL-6, IL-10, IL-12(p70), and IFN-γ were measured in RzCD19Cre mice with B-cell lymphomas (B), T-cell lymphomas (T), and other tumors (mammary tumor, sarcoma, and hepatocellular carcinoma) and in tumor-free RzCD19Cre, Rz, CD19Cr,e and WT mice.

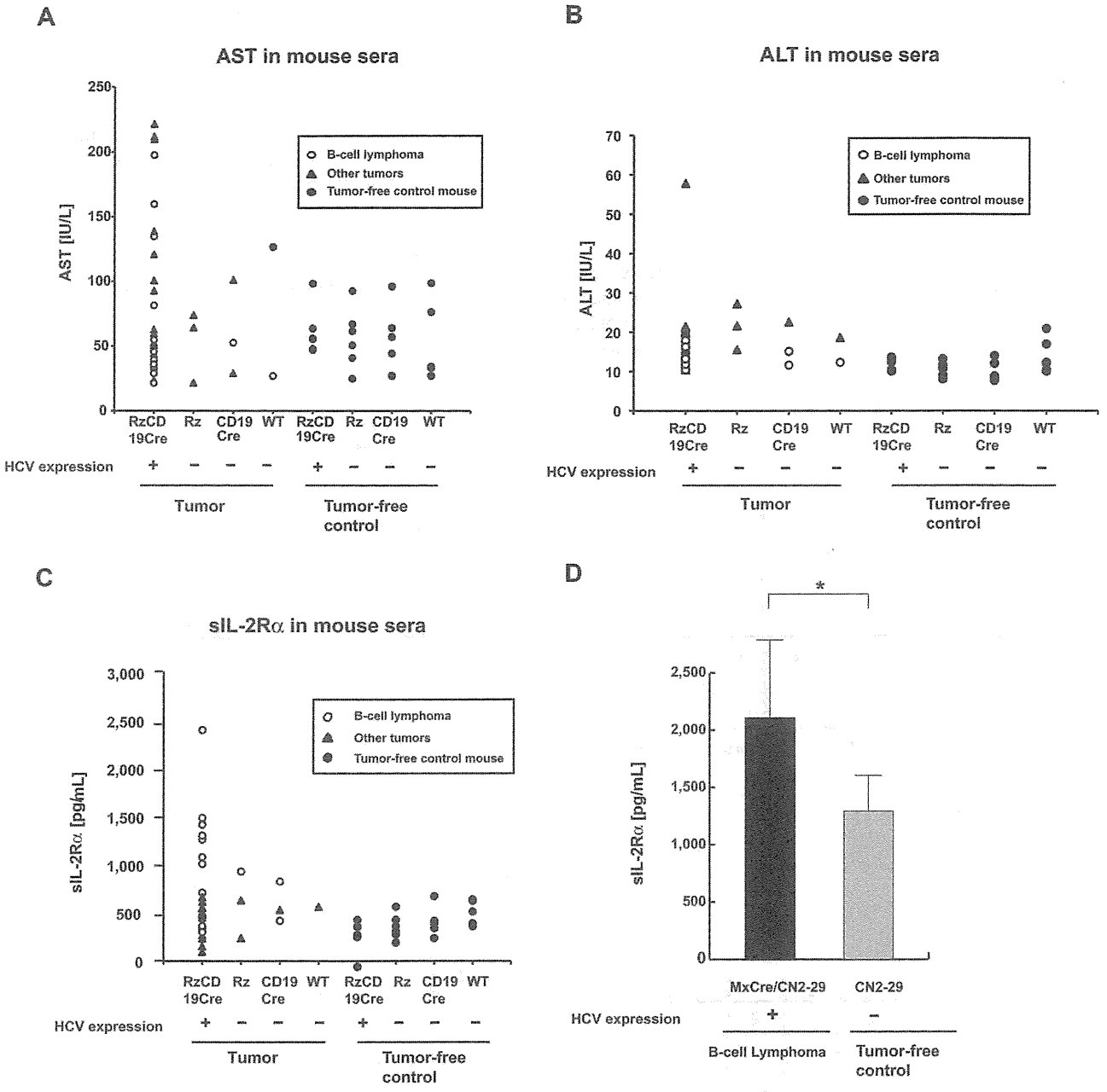

Figure 4. Serum titers of AST, ALT and soluble IL-2Rα in transgenic and control mice lacking or harboring B-cell lymphomas. (A-B) The AST (A) and ALT (B) assays were performed on serum samples from tumor-free control mice and the RzCD19Cre, Rz, CD19Cre and WT mice with or without B-cell lymphomas or other tumors. (C) ELISA analysis was performed to determine the sIL-2Rα concentration in serum samples from tumor-free control mice and the RzCD19Cre, Rz, CD19Cre, and WT mice with or without B-cell lymphomas or other tumors. (D) Concentration of soluble IL-2Rα in sera from transgenic (MxCre/CN2-29 or CN2-29) mice with or without B-cell lymphomas (*$P < .05$).

chronic hepatitis.[29,30] Therefore, we examined tumor cytokine and chemokine levels using a multisuspension array system. The levels of IL-2, IL-4, IL-6, IL-10, IL-12(p70), and IFN-γ (Figure 3), which may have a link with lymphoproliferation[14] or lymphoma[28,31] induced by HCV, and IL-1α, IL-1β, IL-3, IL-5, IL-9, IL-12(p40), IL-13, IL-17, Eotaxin, granulocyte-CSF, granulocyte–macrophage–CSF, KC, monocyte chemotactic protein-1, MIP-1α, MIP-1β, Regulated upon Activation, Normal T-cell Expressed, and Secreted, tumor necrosis factor-α, IL-15, fibroblast growth factor-basic, leukemia inhibitory factor, macrophage-CSF, human monokine induced by gamma interferon, MIP-2, platelet-derived growth factorβ and vascular endothelial growth factor (supplemental Figure 4) were measured in sera from mice with B-cell lymphomas, T-cell lymphomas, and other tumors and in sera from tumor-free RzCD19Cre, Rz, CD19Cre, and WT control mice. The levels of these cytokines and chemokines in sera from tumor-bearing RzCD19Cre mice with B-cell lymphomas were not significantly different from those of the control groups, and thus, changes in the expression of these cytokines and chemokines were not strictly correlated with the occurrence of B-cell lymphoma in RzCD19Cre mice.

The levels of amino transferases and sIL-2Rα in mice lacking or harboring B-cell lymphomas

We also examined the levels of AST and ALT in the RzCD19Cre, Rz, CD19Cre, and WT mice. There were no significant differences in the levels of AST and ALT in the sera of mice lacking or harboring B-cell lymphomas ($P > .05$; Figure 4A-B; AST: